Available online at www.sciencedirect.com
ScienceDirect
ELSEVIER
Palaeogeography, Palaeoclimatology, Palaeoecology 242 (2006) 214–239
PALAEO
www.elsevier.com/locate/palaeo

Calcretes from a Late Quaternary interfluve in the Ganga Plains, India: Carbonate types and isotopic systems in a monsoonal setting

R. Sinha[a,*], S.K. Tandon[b], P. Sanyal[c], M.R. Gibling[d], D. Stuben[e], Z. Berner[e], P. Ghazanfari[b]

[a] *Engineering Geosciences Group, Indian Institute of Technology, Kanpur 208016, India*
[b] *Department of Geology, University of Delhi, Delhi 110007, India*
[c] *Department of Geology and Geophysics, Indian Institute of Technology, Kharagpur 721302, India*
[d] *Department of Earth Sciences, Dalhousie University, Halifax, Nova Scotia, Canada B3H 3J5*
[e] *Institute of Mineralogy and Geochemistry, University of Karlsruhe, 76131, Karlsruhe, Germany*

Received 4 December 2005; received in revised form 6 May 2006; accepted 28 May 2006

Abstract

Calcretes are abundant in Late Quaternary channel and floodplain strata of the southern Ganga plains. In a key section at Kalpi, pedogenic carbonates (nodules, rhizoconcretions, and powdery carbonate) are present within aggradational floodplain deposits, where they correspond to relatively high monsoonal precipitation and river discharge. In contrast, groundwater carbonate has cemented degradational surfaces (discontinuities), which correspond with periods of relatively low precipitation. Mixed groundwater and pedogenic calcretes are present in the deposits of small interfluve channels, and reworked nodules line degradational surfaces and locally fill channels. Most carbonates show alpha fabrics that include floating textures, shrinkage crack fills, and grain coatings. The predominance of alpha fabrics is unexpected, but is characteristic of calcretes across dryland and seasonal parts of northern India, where soil formation led to only weakly developed or poorly preserved beta fabrics.

Interpretation of $\delta^{13}C$ and $\delta^{18}O$ values of bulk and microdrilled calcrete samples suggests relatively little variation in precipitation and vegetation types through the sampled interval at Kalpi. Floodplain deposits were vegetated with a mixture of C_4 and C_3 plants (predominantly C_4), with a higher proportion of C_3 plants associated with channel deposits. This apparent lack of variation is surprising because the sampled interval represents at least 60,000 years of Marine Isotope Stages 3–5, during which climate models suggest that Asia experienced radical fluctuations in monsoon intensity and precipitation. Some of the apparent lack of variation may be explained by preferential preservation of aggradational strata that represent relatively active monsoonal periods, as well as by the mixing of drier floodplain (C_4) and riparian (C_3) vegetation. However, local departures from the regionally based climate model cannot be ruled out. A modest upsection increase in C_4 plants may represent increased aridity and lower atmospheric CO_2.

Isotopic analysis of organic matter from floodplain pedogenic nodules suggests a higher C_3 plant contribution than carbonate-based data would suggest. The preserved organic matter may reflect the annual average biomass in the soil, whereas carbonate formation may have taken place mainly during the drier season when respiration of C_4 plants was more important.

* Corresponding author.
E-mail address: rsinha@iitk.ac.in (R. Sinha).

0031-0182/$ - see front matter
doi:10.1016/j.palaeo.2006.05.015

In interfluve settings such as Kalpi, seasonality may strongly affect the C_3–C_4 system, with preferential preservation of only part of the biomass.

Keywords: Calcrete; Pedogenic and groundwater carbonate; Interfluve; Discontinuity; Carbon and oxygen isotopes; C_4 and C_3 plants; Vegetation; Monsoon precipitation; India; Quaternary

1. Introduction

Many types of carbonate occur in the channel and floodplain successions of modern and ancient river deposits (Friend and Moody-Stuart, 1972; Wright and Tucker, 1991; Tandon and Kumar, 1999; Mack et al., 2000; Nash and Smith, 2003). They include pedogenic, groundwater, mixed pedogenic–groundwater, palustrine and pond carbonates, valley calcretes, and reworked materials. The term "calcrete" has been applied to all of these types, and commonly denotes secondary carbonate introduced into surface and near-surface soil, sediment, and rock through replacive and displacive processes and/or passive cementation (Goudie, 1983). The term is used here to cover a wide range of floodplain and channel carbonates. Such carbonates are common in areas that have a dry climate, as well as in sub-humid areas with a marked dry season, and have been used as paleoenvironmental indicators in alluvial successions, especially for understanding fluctuations in the vadose and phreatic zones. In particular, efforts continue to be made to distinguish pedogenic carbonates from other forms (Tandon and Narayan, 1981; Mack et al., 2000).

A comprehensive model for alluvial carbonate has yet to emerge (Mack et al., 2000). The creation of such a model requires a large amount of information about Quaternary and older alluvial carbonates that represent large and small river systems, as well as for successions from different climatic regimes. A comprehensive model (or multiple models for different climatic–latitudinal belts) is desirable because of the increasing use of pedogenic carbonate as a proxy for atmospheric pCO_2 (e.g. Cerling, 1991; Andrews et al., 1995; Mora et al., 1996; Ghosh et al., 2004), as well as for paleoclimatic and paleoecological reconstruction. The pioneering studies of the Neogene Siwalik Group of southern Asia illustrate the importance of such reconstructions (Cerling, 1984; Quade et al., 1989; Cerling et al., 1989, 1997; Cerling and Quade, 1993; Quade and Roe, 1999). Significantly, Budd et al. (2002) highlighted numerous pitfalls in the use of pedogenic carbonates for these purposes, including overprinting and diagenesis which commonly affect both pedogenic and non-pedogenic carbonates in monsoon-dominated regions. The importance of these effects is magnified where large water-table fluctuations are associated with wet and dry seasons (Tandon and Kumar, 1999).

Despite continuing interest globally in exploiting the potential of alluvial carbonate, surprisingly little is known about the alluvial carbonates of the Ganga Plains in the Himalayan Foreland Basin (see earlier studies by Sehgal and Stoops, 1972; Pendall and Amundson, 1990; Agarwal et al., 1992; Srivastava et al., 1994; Srivastava, 2001). Carbonate accumulations of all kinds, particularly pedogenic and groundwater types, are abundant in this area, and are termed "kankar". This paucity of information is all the more surprising because much of our understanding of alluvial carbonate systems originated from studies of exhumed Himalayan foreland-basin strata of the Siwalik Group.

The present study has two purposes. Firstly, we document from field and microscopic analysis an unusually wide range of carbonate types associated with a Late Quaternary floodplain (interfluve) succession at Kalpi in the southern Ganga Plains. The river cliffs at Kalpi are high and extend for several kilometers, constituting one of the best exposures in the plains, and the carbonates can be placed in a reliable stratigraphic and depositional context. Secondly, we use the carbonates to explore the carbon and oxygen isotopic system of the section, for which an age model spans more than 60,000 years (much of Marine Isotope Stages 3 to 5: Gibling et al., 2005). Because the strength of the monsoon is known from regional climatic modeling to have varied greatly during this period, the carbonate sampling programme was designed to test the response of the isotopic system and vegetation to precipitation changes. Surprisingly, there is only evidence in our data for modest changes in the isotopic system and vegetation meaning either less precipitation variation than implied by climatic models, or less forcing of

precipitation on the isotopic and vegetation systems. Local departures from the general climatic model are possible. However, we suggest that the results have been affected also by preferential sampling of short aggradational periods that represent a restricted climatic condition, as well as by the presence of local riparian (river-related) vegetation within a drier biome. Our results have implications for the interpretation of isotopic data in alluvial settings.

2. Regional framework

2.1. Geographic setting

The study area lies within the southern part of the Himalayan Foreland Basin, about 500 km south of the Himalayan mountain front and about 1200 km inland of the modern tidal limit of the Bay of Bengal (Fig. 1a). The area presently experiences a sub-tropical, monsoonal

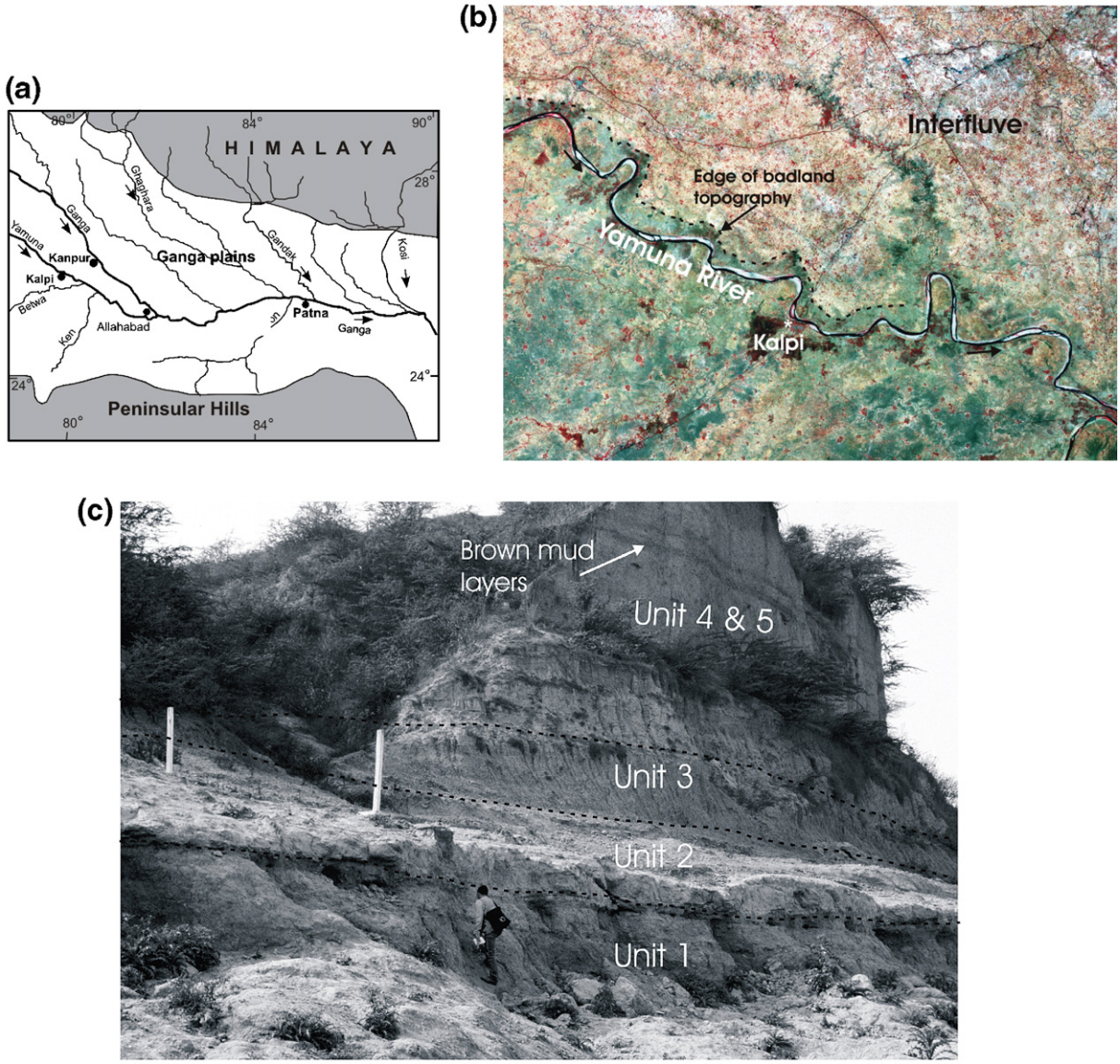

Fig. 1. (a) Location map of the study area near Kalpi in the southern Ganga Plains of India. (b) Satellite image shows distinct badland areas (darker grey shades) on both sides of the Yamuna River but especially on the southern side. Paler grey areas farther from the river denote a slightly dissected interfluve surface. The studied section lies on the southern bank where the Kanpur–Orai road (NE–SW line) crosses the river on a bridge. Bajpai and Gokhale (1986) and Sinha et al. (2002) provided detailed geomorphic descriptions based on satellite images. (c) Southeastern part of the cliff section (33 m high at its maximum), which is divided into 5 stratigraphic units (see text).

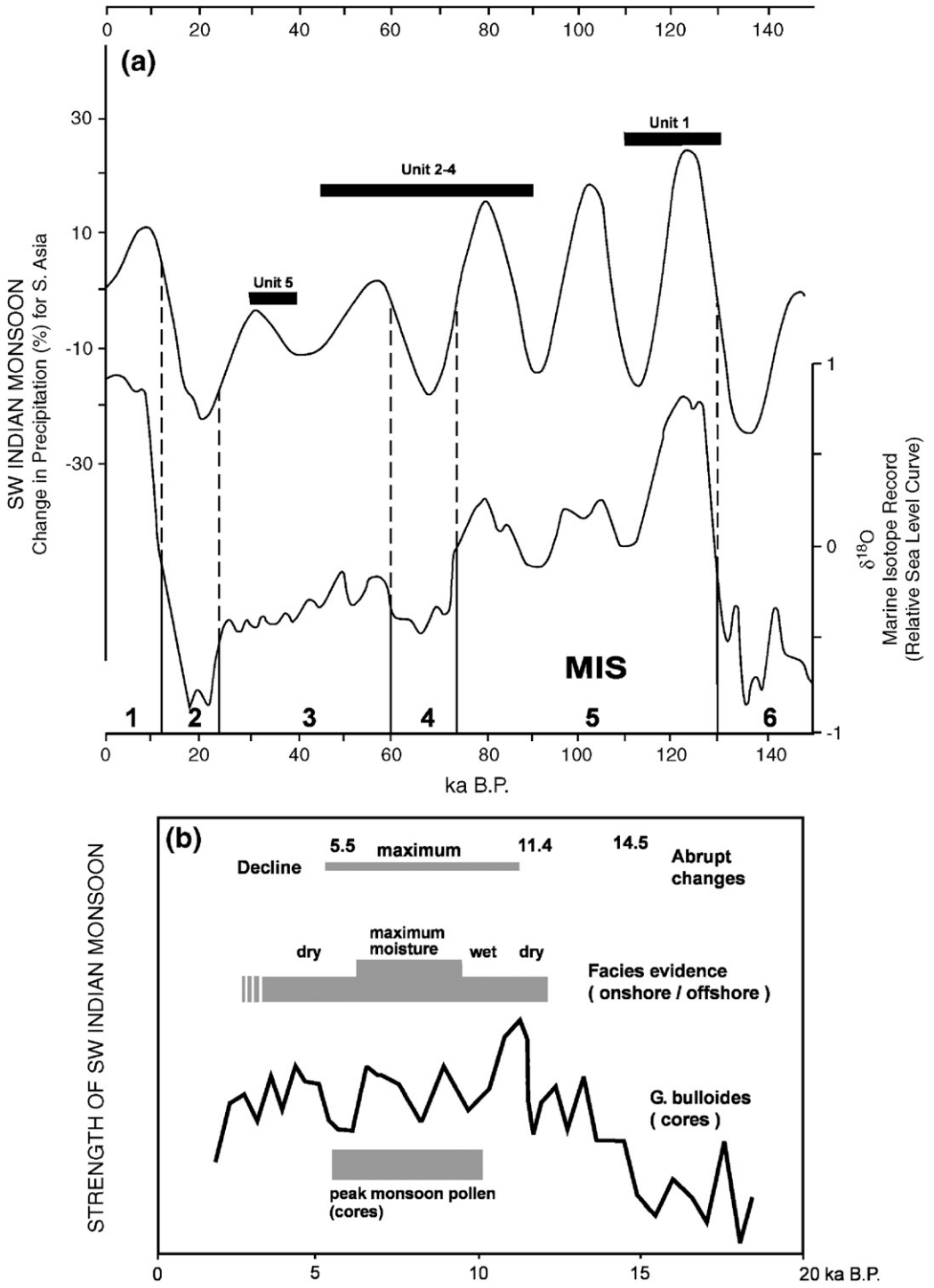

Fig. 2. Variation in precipitation associated with Southwest Indian Monsoon. (a) Modeling results for the past 150 ka, from Prell and Kutzbach (1987), shown in relation to proxy eustatic curve (Waelbroeck et al., 2002). MIS=Marine Isotope Stage. (b) Major trends in precipitation for the past 20 ka, from Overpeck et al. (1996). Geological information includes facies evidence from dated sections in the Arabian Sea and onshore in Asia, and the abundance of *Globigerina bulloides* and African pollen (linked to wind strength and upwelling) from Arabian Sea cores.

regime, with average precipitation of 800–1000 mm/year, mean maximum temperature of 30–32 °C, and mean minimum temperature of 15–18 °C (Singh, 1994). The maximum temperature in the summer frequently exceeds 45 °C and the minimum temperature in winter occasionally drops below 2 °C. The monsoon typically arrives in mid-June preceded by pre-monsoon showers, and provides more than 85% of the annual rainfall through to September.

The study area constitutes part of the interfluve between the Yamuna and Ganga rivers, which is about 75 km wide in this region and mostly beyond the reach of the highest floods on these two big rivers (Kale, 1998), which are deeply incised. The interfluve is above 130 m above mean sea level near Kanpur, and decreases in elevation southeastward, with relief on a traverse across the interfluve of only a few meters. Brickpit sections up to 2 m thick in the interfluve commonly show brown floodplain clays with carbonate nodules and interbeds of yellow-brown silt. Previous investigations (Agarwal et al., 1992; Srivastava et al., 1994; Srivastava, 2001) have reported widely occurring and patchy kankar deposits in the shallow sub-surface, in layers up to 1 m thick and as scattered centimeter-scale nodules. Soils in this area are mainly typical Haplustepts, with local fluventical and vertical Haplustepts and Fluvaquents (D.K. Pal, written communication, 2003).

The Kalpi section is located on the bank of the Yamuna River, where a NW–SE oriented cliff nearly 1500 m long exposes 33 m of strata along the southern bank at low-flow stage (Fig. 1b, c). Alluvial bars flank a narrow active floodplain on the northern bank. On the remote sensing image (Fig. 1b), "badland topography" is the most distinctive landform near the cliff (Sinha et al., 2002), and is characterized by intensive gully erosion of strata equivalent to those in the cliff and variable but locally dense vegetation cover. The cliff top is not an active floodplain, although the river level approaches the cliff top during exceptional monsoon seasons. Badlands extend for up to 3 km on either side of the Yamuna, and their limit is marked by an irregular but distinctive boundary (Fig. 1b) that reflects the extent of headward erosion. The badland terrain lies on average about 20 m above the low-stage river level, with a progressive increase in elevation of about 10 m to an inactive but only slightly dissected interfluve surface. This extensive level has scanty vegetation and a few small channels that rise on the interfluve (plains-fed rivers).

The exposed cliff strata belong to the Older Alluvium (Bhangar), one of two morphostratigraphic units recognized for the Ganga Plains (Pascoe, 1917; Narula et al., 2000). The Newer Alluvium (Khadar) occupies the modern river valleys. Singh et al. (1999) briefly described the Kalpi section and divided the strata into three "events" (I–III) that correspond broadly with Units 1, 2 and 3–5, respectively, of the present study. Age dates (see below) indicate that the bulk of the strata in the Kalpi section are in the age range of ~35 to 120 ka, and thus the section represents an exceptionally fine Late Quaternary "window" through southern Ganga interfluve deposits, spanning a substantial proportion of the period between the last and penultimate glacial periods (MIS 2 and MIS 6, respectively).

2.2. Long-term record of the monsoon

The Southwest Monsoon exerts a dominating influence on the Ganga Plains. The strength of the monsoon, which is affected by solar insolation patterns and glacial boundary conditions (Prell and Kutzbach, 1987; Clemens et al., 1991), has been modeled in detail for the Late Quaternary of southern Asia (Prell and Kutzbach, 1987, 1992; Anderson and Prell, 1993; Overpeck et al., 1996). Precipitation changes are estimated to have been as much as ±30% regionally over the past 150 ka (Fig. 2a).

Although model-based estimates provide only a general assessment of local precipitation, field-based estimates have broadly confirmed the model results, especially for the past 30 ka for which there is good stratigraphic coverage. The lowering of precipitation predicted for the Last Glacial Maximum (Marine Isotope Stage 2) is demonstrated from the presence of lakes and eolian dunes in parts of the Ganga Valley after about 27 ka (Gibling et al., 2005). The predicted intensification of the monsoon during Marine Isotope Stage 1 (Fig. 2b) is evident in northwest India where precipitation at about 10 ka was twice the present values (Swain et al., 1983), with a corresponding increase in sediment flux to the Ganga–Brahmaputra delta in the 7–11 ka period (Goodbred and Kuehl, 2000). Goodbred (2003) presented compelling evidence that secular variation in Southwest Monsoon precipitation has influenced water and sediment discharge in the Ganga system over the past ~60 ka, affecting patterns of aggradation and degradation from source to sink.

3. Methods

Serial photographs of the 33 m cliff section were combined to form a photomosaic, from which a detailed

tracing of the strata was constructed. The tracing allowed five stratigraphic units to be correlated along the cliff (Figs. 1c and 3) and their thickness and facies variation recorded. The lithology of the units was documented from 13 stratigraphic logs, supplemented by notes at intervening localities and in gullies behind the cliff (Figs. 3 and 4).

The varied types of carbonate were classified, and samples were collected from each stratigraphic unit, mainly from three sections, log II, III and IX (see Fig. 4). Some of the carbonate veins (described later) cutting across the stratigraphic units were also sampled for isotopic analysis. Thin sections were prepared from carbonate samples for petrographic study. From a comparable set of thick sections (80 μm thick) that closely matched the thin sections, microdrill samples were extracted from specific types of carbonate material under the binocular microscope, and analysed for stable isotopes. This procedure was conducted in order to address to some extent the concerns expressed by Budd et al. (2002). The correspondence between isotopic data obtained from these two sources is reasonably good.

Carbon and oxygen isotope analysis of 38 bulk and 27 microdrilled carbonate samples employed an automated carbonate preparation system (MultiCarb) connected on-line to an isotope ratio mass spectrometer (Optima, from Micromass UK Ltd.) at Institute of Mineralogy and Geochemistry, University of Karlsruhe, Germany. In addition, 10 vein samples were analysed at Geochron Laboratory at Cambridge, MA. The preparation line was based on the standard method by measuring the isotope ratios in CO_2 released by reaction of the carbonate with 100% phosphoric acid. Samples were reacted in individual vials, eliminating the risk of cross-contamination from one sample to the next. Isotopically calibrated CO_2 pressure bottles from Messer Griesheim, Germany, were used as reference gas. Instrumental precision was $<0.008‰$ for $\delta^{13}C$ value and $<0.015‰$ for $\delta^{18}O$ value. Accuracy was checked with the limestone standard NBS-19. Isotopic results are given in ‰ deviation relative to V-PDB reference values.

For analysis of organic matter, powders from 11 nodules (after screening for modern rootlets) were treated with 0.5 N HCl to remove carbonate, rinsed with distilled water 5 to 6 times and finally combusted under vacuum at 800 °C in the presence of cupric oxide and silver foil for 6 h to release CO_2. The CO_2

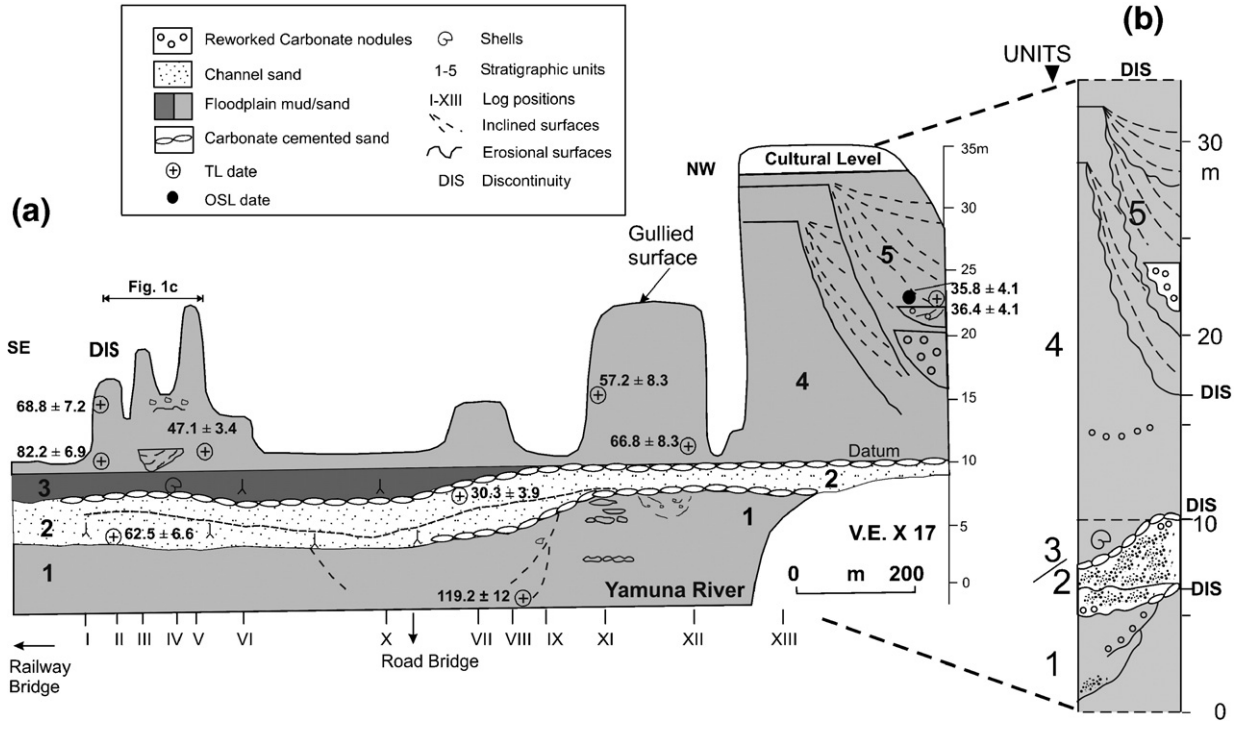

Fig. 3. (a) Stratigraphic profile of the Kalpi section based on 13 logs; note that at high cliff section at location XIII, thicknesses of different units could not be measured but were estimated. (b) Summary log of Kalpi section showing 5 stratigraphic units separated by discontinuities.

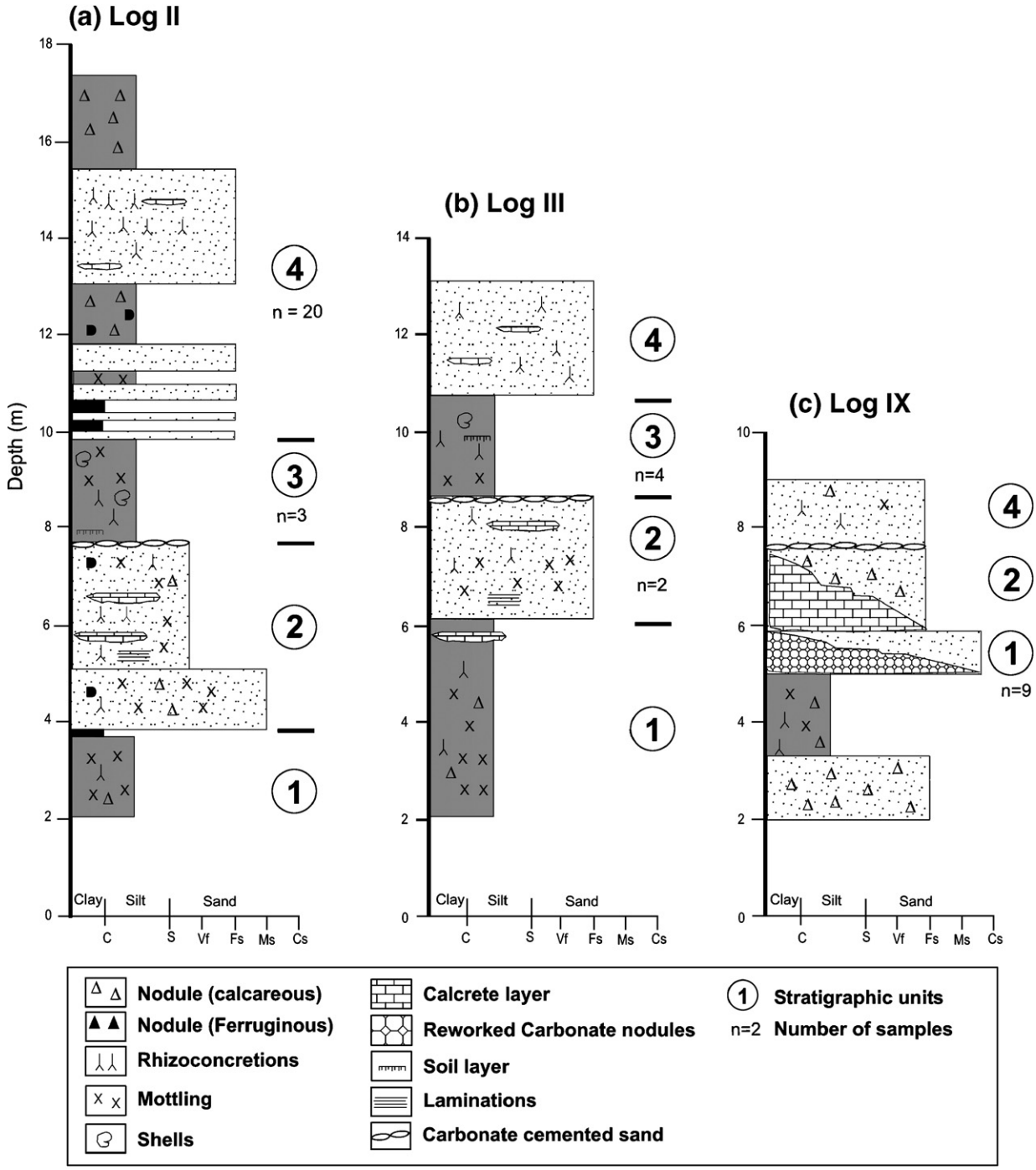

Fig. 4. Detailed lithologs from selected locations showing sample points for petrographic and isotopic analysis (see Fig. 3a for exact location of lithologs). (a) Log II, samples are from Unit 3 (II/3.1 to 3.2) and Unit 4 (II/4.1 to 4.16). (b) Log III, samples are from Unit 2 (III/2.1 to 2.2) and Unit 3 (III/3.1 to 3.4); (c) Log IX; all samples are from Unit 1 (IX/1.1 to 1.9).

was separated and purified cryogenically and stable isotope ratios were measured using a Europa Geo 20–20 mass spectrometer. To check the reproducibility of measurements, IAEA C-3 cellulose standard ($\delta^{13}C$: −24.5‰) was analyzed along with each set of samples.

4. Kalpi section

4.1. Stratigraphic units and paleoenvironmental interpretation

Details of the stratigraphic units in the Kalpi section (Fig. 2) and lithofacies interpretations are given in Gibling et al. (2005). The units are outlined here with special emphasis on carbonate materials, the megascopic and microscopic appearance of which are described more fully below. The Kalpi section includes a wide range of carbonate types, and also appears representative of types noted in several other smaller sections in the southern Ganga Plains (Gibling et al., 2005; Sinha et al., 2005a,b).

The basal Unit 1 consists of at least 6.6 m of floodplain deposits (Gibling et al., 2005), represented by red-brown silty clay with discontinuous horizons of rhizoconcretions (growth of carbonate around living or dead plant roots: Klappa, 1983) and carbonate nodules, as well as disseminations of whitish powdery carbonate. Drab mottles indicate that the muds were affected by pedogenesis, and the presence of drab mottles and rhizoconcretions testifies to the former presence and decay of vegetation. Carbonates and subordinate Fe/Mg segregations within the paleosols suggest seasonal climates. Rhizoconcretions are concentrated at some levels, but horizonation is weak and no sesquioxide horizons indicative of sustained soil formation were noted. Medium-grained sand at the base of the section represents a channel fill.

In the upper part of the unit in the north-western part of the section (log IX and beyond: Figs. 3 and 4), degradation of the floodplain deposits generated gully fills, at least 6 m thick, that contain lenses of reworked carbonate gravel on inclined surfaces. The top of Unit 1 represents a prominent discontinuity, and is marked by an irregular surface of carbonate-cemented sand with a patchy distribution, locally overlain by carbonate gravel (Fig. 5a). The carbonate-cemented layer follows a degraded paleosurface (between Units 1 and 2) that represents a former erosional landscape. The cap of carbonate gravel indicates that cementation took place at a depth shallow enough for erosional reworking.

Unit 2 is up to 4.2 m thick and consists of two superimposed channel bodies (each up to 3 m thick) that represent small, plains-fed rivers (Gibling et al., 2005). The lower channel body consists of sand sheets and lenses (Fig. 3) with distorted stratification (possibly indicative of seismically induced dewatering) above a basal lag of reworked carbonate gravel. The sand contains abundant carbonate in the form of rhizoconcretions (especially prominent in the upper parts: Fig. 5b), nodules (some coated with pyrolusite), and ball-like masses of cemented sand (Fig. 5c), as well as some Fe/Mn nodules. Rhizoconcretions and carbonate nodules are also prominent in the upper channel body. The abundance of rhizoconcretions indicates that vegetation was a prominent feature of the landscape during and/or following channel deposition, and the varied carbonate types suggest both pedogenic and groundwater cementation in this unit.

A prominent carbonate-cemented sand caps the upper channel body of Unit 2 (Figs. 3 and 4). The sand fills scours on a gullied surface and is associated with lenses of cross-bedded carbonate gravel. These features indicate that the unit top marks a strong discontinuity, and the cemented surface also suggests phreatic and capillary zone cementation of a gullied palaeosurface (groundwater origin). Many carbonate veins cut Units 1 and 2 (Fig. 5d), and are inferred to represent joints generated by seismic action and later cemented by carbonate from groundwater systems. The seismic event predated Unit 3, which is not cut by the veins.

Unit 3 comprises 3 m of floodplain sediment (Gibling et al., 2005) that fills an extensive hollow on top of Unit 1 (Fig. 3). It consists of unstratified clay-rich mud with gastropods and bivalves at one locality. Other features include rhizoconcretions (Fig. 5e), small carbonate nodules, dark Fe/Mn patches, and vertical drab mottles, with a few slickensides. Patches of relict stratification imply that the muds have been intensively destratified, and a locally prominent vertical fabric is associated with vertically elongate rhizoconcretions and carbonate sheets, suggestive of vertical, shrink–swell effects. Pedality is weakly developed. These features collectively indicate that the Unit 3 muds have undergone strong pedogenesis.

Unit 4 comprises a thick (23.3 m) succession of interbedded mud and sand that rests gradationally on Unit 3, from which it is demarcated by the incoming of sand sheets. It is best exposed in the large cliff in the northwest area, although it was most fully examined in shorter, accessible logs (II–V; Figs. 3 and 4) and in gullies behind the cliff face. The unit comprises sheets of silt and sand interbedded with mottled and bioturbated brown mud; two prominent, closely spaced brown muds (Fig. 1c) can be traced for at least 200 m in the southeastern cliffs. Rhizoconcretions, small nodules, and soft carbonate patches are common, and large carbonate nodules form discontinuous bands in the lower part. Small dark nodules and red ferruginous, millimeter-sized nodules are present locally.

Fig. 5. Field photos of carbonate occurrences in the Kalpi section. (a) Carbonate-cemented sand marks an irregular surface of discontinuity at the top of Unit 1. Note the inclined surfaces mantled by carbonate gravel in the underlying muds, which mark gully fills. Exposed section is 4 m thick. (b) Cylindrical branched rhizocretions in the channel sand of Unit 2. Exposed section is 1 m thick. (c) Ball-like mass of cemented sand at the top of Unit 2. (d) Fracture filled with carbonate sheets cutting Units 1 and 2. (e) Unstratified, clay-rich mud of Unit 3 with rhizocretions. (f) Large gully fills of Unit 5 showing cross-stratified layers of carbonate gravel.

Unit 4 represents the accumulation of thick, extensive floodplain sand and mud sheets (Gibling et al., 2005) above the muddy backswamp deposits of Unit 3. The basal sand layer suggests the invasion of the backswamps by crevasse splays or levee sheets. A modest degree of pedogenesis is evident from mottling, carbonate and ferruginous nodule formation. One layer of reworked carbonate indicates that at least one period of floodplain degradation intervened during the deposition of this predominantly aggradational unit.

Unit 5 represents three episodes of gully cutting and filling (Gibling et al., 2005), with gully filling up to 10 m thick (Fig. 3) and composed largely of colluvial material (Fig. 5f). It is of relevance here to note that one gully fill includes two (largely inaccessible, NW end of the cliff, Fig. 3a) lensoid channel bodies up to 5 m thick, composed of cross-stratified carbonate gravel. These indicate that the gullies were locally sites of throughgoing drainage.

4.2. Age of strata

A summary account of the age of the strata is given in Gibling et al. (2005) and the ages are shown in Fig. 3a. Because dated samples from the upper part of Units 4 and 5 were the only samples to yield finite dates based on optically stimulated luminescence (OSL) of quartz, the older units have been dated using thermoluminescence (TL) ages of quartz. Excellent correspondence was obtained between TL and finite OSL dates in Units 4 and 5, confirming the validity of this approach to dating the section. The units can be correlated broadly with Marine Isotope Stages (MIS). The age of the carbonate materials could not be determined directly. Srivastava et al. (2003) dated the base of the section to 76±11 ka and cliff-top strata to 32±5 ka using OSL methods.

Based on these dates, the Kalpi cliff section is inferred to span part of the Late Quaternary (MIS 3–5), and may perhaps extend into the Mid-Quaternary (>125 ka). In view of the large error bars for the OSL and TL dates, as well as one apparently anomalous date, the age model for the section is only broadly constrained. Nevertheless, if error bars are taken into account, the sampled interval of ~18 m probably represents a period of 60,000 to 90,000 years, spanning part or all of three marine isotope stages.

4.3. Discontinuity-bounded units

A key feature of the Kalpi section, as well as other sections in the region (Williams and Clarke, 1995; Gibling et al., 2005; Sinha et al., 2005a) is the prominence of erosional discontinuities. The stratal architecture is that of discontinuity-bounded units (sequences) that represent alternate phases of floodplain aggradation and degradation (Fig. 3b). The discontinuities between Units 1 and 2 and Units 2 and 3 are marked by erosional relief, calcite cementation, and paleosols. Because of limited exposure, the areal extent of the units and discontinuities is not known, but those in the Kalpi section can be traced for the full cliff length of 1.5 km (Fig. 3a).

Discontinuities such as these may reflect floodplain gullying and headward erosion associated with incision along major drainage lines. Based on facies in exposed sections and age models, Gibling et al. (2005) reasoned that the discontinuity-bounded sequences are tracking climatic changes on the scale of marine isotope stages (10^4 year timescales). The sequences are probably related to large fluctuations of monsoonal precipitation (Prell and Kutzbach, 1987), leading to large variations in river discharge and sediment transport. These variations reflect the hydrological response of upland catchment systems to monsoonal strengthening and weakening, supplemented by drainage from the local plains.

5. Carbonate types: field and petrographic characteristics

5.1. Classification

Eight types of carbonate (Table 1) are distinguished on the basis of megascopic physical appearance (size and form), host sediment (sand or mud), degree of induration (indurated or powdery), relationship to discontinuities and tectonic structures, and petrographic character.

Indurated, sub-equant nodules, a few centimeters in diameter, are common in all the Kalpi units, where they are disseminated or concentrated in discontinuous zones. This carbonate is the most abundant type in the southern Ganga plains alluvium, based on outcrops and drill cores, and commonly ranges from a few percent to 20% by volume of floodplain deposits. In view of the poor development of internal layering, the bodies are termed “nodules” rather than “concretions” (Brewer, 1964). The petrographic features of nodules in sandy or muddy sediment were studied separately. Powdery carbonate and rhizoconcretions, are also common, although they rarely form more than a few percent of the floodplain deposits. These types are composed predominantly of micrite with local sparry patches, and

Table 1
Classification of carbonate types in the Kalpi section

Carbonate type	Genetic type	Stratigraphic occurrence
1. Carbonate hosted in sand		
1.1. Nodules	Mixed pedogenic-groundwater	Units 1, 4
1.2. Rhizoconcretions and ball-like masses of cemented sand	Mixed pedogenic-groundwater	Unit 2
1.3. Groundwater-cemented sand (nodular and brecciated-irregular cemented sandy horizons associated with discontinuities)	Mixed groundwater-pedogenic	Units 1 to 4 (Units 1–2 and 2–3 boundaries)
2. Carbonate hosted in mud		
2.1. Nodules	Pedogenic	Units 1, 2, 3
2.2. Rhizoconcretions	Pedogenic	Units 1, 2, 3, 4
2.3. Powdery	Pedogenic	Unit 1
3. Fracture fill (vein fills) (cemented sandy silt, in places nodular appearance)	Vadose/Groundwater (?)	Cross-cutting Units 1 and 2
4. Reworked carbonate nodules	Sheet flow/Channel flow	Units 1 and 2

the setting and petrographic character of all these types suggests that they are predominantly pedogenic.

Cemented sand and ball-like masses of cemented sand occur as sheets and lenses along discontinuities at Kalpi and elsewhere, and are interpreted as non-pedogenic, formed through the influence of groundwater. The carbonate is predominantly sparry, and shrinkage-related fabrics, alveolar fabrics, and clotted micrite are largely absent. Also attributed to groundwater are vein fills, which are common in the lower part of the Kalpi section but rare elsewhere in the region. Reworked carbonate nodules are associated with both pedogenic and non-pedogenic carbonates at numerous levels.

5.2. Carbonate hosted in sand

5.2.1. Nodules

Three types of calcite are observed within the nodules. Mosaics of subhedral calcite, with thicker zones between subhedral crystals, indicate re-precipitation along dissolutional boundaries (cf. Tandon and Kumar, 1999). Areas of calcite spar have incorporated detrital grains which have etched margins and appear to be floating (Nagtegaal, 1969; Watts, 1978). Thirdly, patches of micrite and microspar are present, with the micrite crystals of uniform size in any patch but varying in size from patch to patch.

5.2.2. Rhizoconcretions and ball-like masses of cemented sand

These two types are intimately associated in Unit 2. Cylindrical, branched rhizoconcretions are typically 1–5 cm in diameter but up to 30 cm in diameter. They consist of dark micrite with detrital grains (Fig. 6a). Some root-related fabrics resemble alveolar fabrics (Esteban and Klappa, 1983; Wright and Tucker, 1991), and networks of spar-filled microchannels of varied size have micritic walls (Fig. 6b).

Ball-like masses of cemented sand are present in both Unit 2 channel bodies, where the ‘porous’ sand has probably contributed to the growth of large nodules. Masses within the lower body show a crisscross vein network of calcite. Lenses of carbonate-cemented sand cap the upper body, and fill scours on a gullied surface that extends for the length of the outcrop. Thin sections reveal detrital grains floating in a carbonate groundmass (Fig. 6b). In grain-rich areas, micrite shows a patchy distribution and is locally rusty-brown. Micrite-dominated areas show local patches of spar that were variably shaped open spaces in which calcite precipitated, mostly as subhedral mosaics.

Fig. 6. Photomicrographs of carbonate materials under crossed nicols (except for plane-polarised light in (a)). (a) Vertically elongate rhizoconcretion (Unit 2), composed of micritic micronodules and spar-filled microchannels, with floating fabric of detrital grains. (b) Photomicrograph of rhizocretion of Unit 2 showing dark micrite with abundant floating grains. Chambers, microchannels and lacy networks filled by spar are observed. These resemble alveolar fabric (X-nicols). (c) Carbonate-cemented masses in brown sand of Unit 2 showing a grain-dominated area of angular/sub-angular quartz grains. Note the development of calcite spar areas in the lower left and upper right. (d) Photomicrograph of nodule of muddy layer of Unit 4 showing floating grain of quartz and feldspar in micrite. Local development of spar patches is observed (X-nicols). (e) Rhizoconcretion developed in Unit 1 muds. Fragmented nodules and grain-dominated areas are clearly demarcated. Note the development of bladed spar at the boundary of these two areas. (f) Rhizoconcretion (Unit 1) showing development of shrinkage features. Note the growth of spar crystals from the margin of shrinkage spaces. (g) Nodules in powdery carbonate within silty mud (Unit 1). Nodules consist of micrite, with common segregation of micrite to spar. (h) A grain of *Microcodium*(?) in a reworked carbonate fragment in Unit 1.

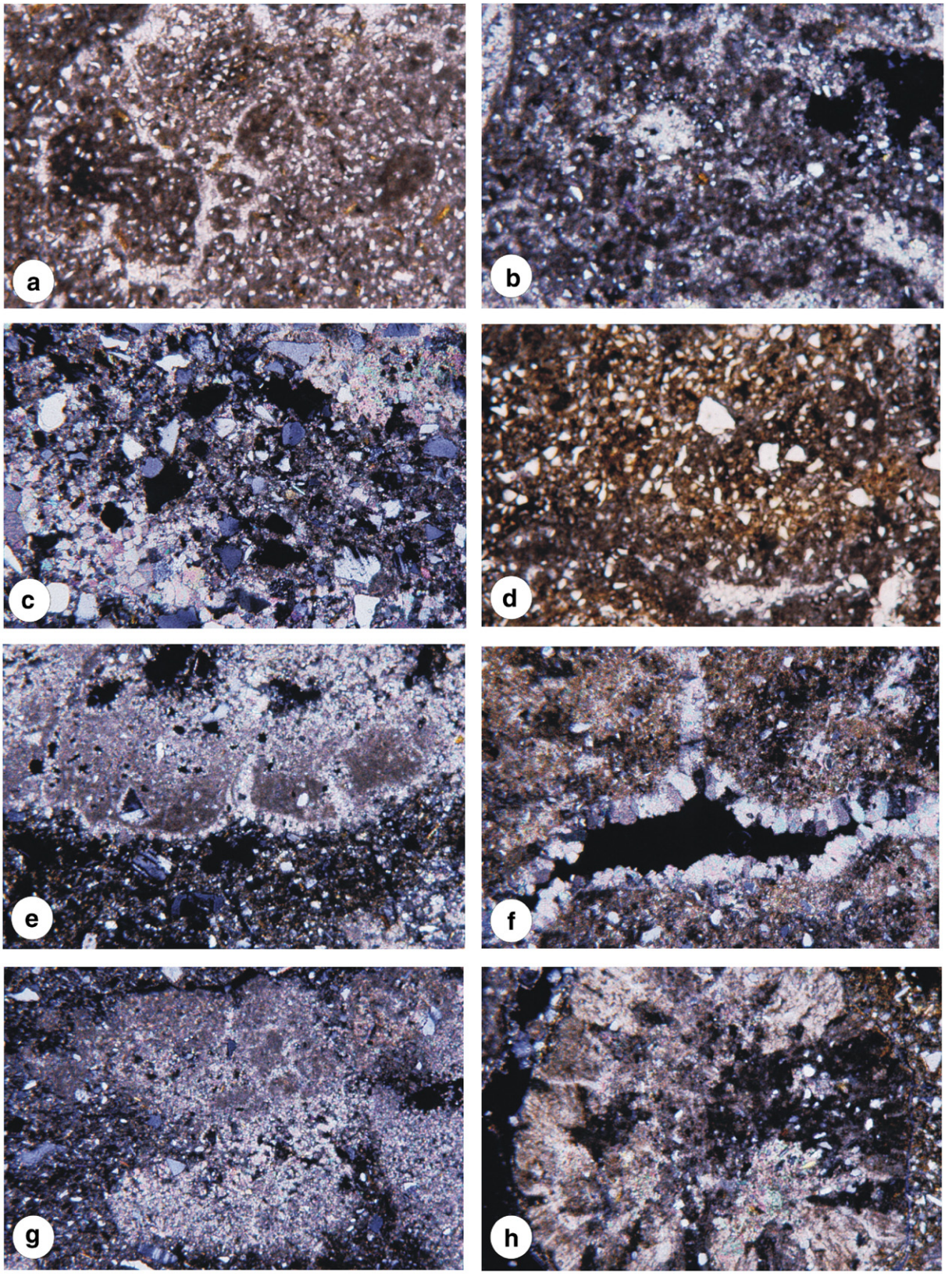
a
b
c
d
e
f
g
h

5.2.3. Carbonate-cemented sand

The irregular discontinuity at the top of Unit 1 is marked by several decimeters of carbonate-cemented sand with local carbonate gravel (Fig. 3a,b). In places, the cemented material appears nodular and brecciated. A less pronounced nodular-cemented layer is also present at the Unit 2/3 discontinuity. Thin sections show abundant floating grains (mainly quartz) in a spar groundmass, with some spar mosaics that may represent cavity fills (Fig. 6c).

5.3. Carbonate hosted in mud

5.3.1. Nodules

Nodules developed in mud predominate in the Kalpi section. Nodules in Unit 3 represent a homogeneous carbonate impregnation of the host sediment. Micritic areas vary from light to dark brown, and mica platelets are present. Linear unfilled spaces may be shrinkage related. Nodules in Unit 4 have a predominantly micrite groundmass, with abundant silt-sized quartz and a few larger plagioclase and quartz grains, as well as some opaque grains (Fig. 6d). One large micrite 'pedorelict' (Bullock et al., 1985) has alveolar structure. Spar-micrite intergrowth areas are present, as well as local patches of micrite admixed with clay. A few nodules are slightly reddened, indicative of local mobility of iron.

5.3.2. Rhizoconcretions

Rhizoconcretions are common in muddy Units 1, 3 and 4 (Fig. 5b, e). Those in Unit 1 are cylindrical and tubular, and have surface nodes. Within the dark floodplain muds of Unit 3, the rhizoconcretions include cylindrical, branched, globular and botryoidal forms, and are closely associated with vertical sheet- to rod-like calcareous features that are probably shrinkage-related.

Rhizoconcretions from Unit 1 consist of micrite and microspar, with concentrated or scattered quartz grains, and relatively fresh microcline. The boundary between the calcareous and detrital areas is marked by bladed spar (Fig. 6e) that may have filled open spaces. Additionally, several microspar-spar areas display a sucrosic fabric. Shrinkage cracks filled by spar (Fig. 6f) are common (cf. Tandon and Friend, 1989; Tandon et al., 1998).

Rhizoconcretions from Unit 3 consist of dark micrite with floating grains of quartz, mica and a few feldspars. Poorly developed alveolar structures display unconnected microchannels filled by tiny microspar and spar crystals. Rusty brown mud patches or fragments show envelopes of elongate spar crystals. Pockets of silt-sized quartz and mica may have filled voids.

5.3.3. Powdery carbonate

Within Units 1 and 4, millimeter-sized patches of whitish powdery carbonate are present in the gleyed and grey-mottled zones of massive silty mud, where they are associated with millimeter-sized carbonate nodules. Thin sections show carbonate-impregnated disorthic nodules (Fig. 6g) with abundant floating detrital grains that commonly have etched margins. Nodules consist of micrite with local neomorphic aggradation of micrite to spar (cf. Tandon and Friend, 1989). Framework grains include large polycrystalline quartz, feldspar (larger than the quartz), abundant oriented mica flakes, and opaque grains.

5.4. Fracture fills (vein fills)

Near-vertical calcite sheets, 1–5 cm wide (Fig. 5d), cut Units 1 and 2 all along the exposure. On bedding surfaces, the sheets are straight to curvilinear with anastomosing networks that have amalgamated with rhizoconcretions. Some sheets can be traced for 10 m along strike, and individual veins extend vertically for at least 6 m, down to the river level. Similar veins several meters in vertical extent are present in Quaternary sections elsewhere in the southern Ganga Plains (Sinha et al., 2005b).

5.5. Reworked carbonate nodules

Reworked carbonate fragments are prominent in modern channels, in paleochannel fills, and on gullied floodplain surfaces across the southern Ganga plains. In some paleochannel fills, they form virtually the entire gravel component with few extrabasinal clasts (Sinha et al., 2005b). At the top of Unit 1 (log IX and westwards: Fig. 3), large gully fills contain reworked carbonate fragments up to 2 cm in diameter, concentrated in scour fills on inclined surfaces. Near log 1, Unit 2 channel sand has a basal lens of carbonate gravel with clasts up to 4 cm in diameter (average 0.5 cm), and lenses of cemented, cross-bedded carbonate gravel mark the gullied top of the unit. A layer of reworked gravel (<1 cm fragments) was observed within Unit 4, and channel fills of reworked carbonate (<2 cm fragments) are present within Unit 5. Reworked nodules in Unit 1 are mostly micritic, although somewhat variable in crystal size. Spar-filled microcracks and microchannels are common, and one grain of *Microcodium* (?) was noted (Fig. 6h).

5.6. Carbonate genesis and environmental implications

In pedogenic calcretes, alpha and beta fabrics are considered as petrographic (micromorphological) end members, with many calcretes exhibiting mixtures of the two (Wright and Tucker, 1991). Nash and McLaren (2003) pointed out that calcretes formed predominantly by soil-forming processes exhibit beta fabrics with strong evidence of biological activity (cf. Wright and Tucker, 1991). Such beta calcretes are considered to be best developed in vegetated semi-arid to sub-humid belts.

Despite the above observations, most fabrics documented in this study, including those from nodules, rhizoconcretions, powdery carbonate, reworked nodules, and many groundwater calcrete, are of alpha type (e.g. Tandon and Narayan, 1981; Wright and Tucker, 1991). Distinctive fabric elements include floating textures, micrite–microspar patches, nodule development, calcite cement (passively precipitated in shrinkage spaces), grain-coating micrite, and bladed spar on the walls of shrinkage spaces. This suggests that the calcretes formed mainly through evaporation or evapotranspiration and degassing, with limited biological activity. Microbes present in root systems may have played some role in carbonate precipitation as has been demonstrated by Monger et al. (1991).

Some rhizoconcretions and calcareous sandstone masses show alpha-type fabrics, with some weakly developed alveolar fabrics in the form of spar-filled microchannels with walls of micrite (Fig. 6b), as well as one probable *Microcodium* grain (Fig. 6h). Apart from these cryptic indications of beta fabrics, no other evidence has been recorded. Fabric elements that were searched for but not recorded include calcified filaments, needle fiber calcite, microbial tubes, root mats, and calcified faecal pellets (Bal, 1975; Klappa, 1978, 1979; Mount and Cohen, 1984; Wright and Tucker, 1991; Verrecchia and Verrecchia, 1994).

Carbonate-cemented sandstones (non-pedogenic calcrete) show an irregular appearance, partly because they are related to gullied surfaces. They mainly consist of intergranular spar and cavity-filling spar. In terms of their micromorphology, they are a relatively uniform group, in contrast with pedogenic or mixed-origin alpha calcretes in the sample set and are interpreted as groundwater calcretes. Sparry cement predominates in groundwater calcrete associated with the interfluve channels of Unit 2, resembling groundwater calcretes of the Siwalik Group (Tandon and Varshney, 1991; Quade and Roe, 1999). They consist largely of intergranular spar cement and have floating-grain textures, with no indication of beta fabrics.

In summary, pedogenic nodules in the Kalpi section show a predominance of alpha fabrics, whereas rhizoconcretions and calcareous sandstone masses include some weakly developed alveolar fabrics. Pedogenic calcretes are associated with aggradational floodplain deposits (Units 1, 3, and 4), and probably correspond with periods of relatively high monsoonal precipitation and river discharge. In contrast, cemented degradational surfaces along discontinuities (boundaries of Units 1 and 2, and 3 and 4) probably correspond to periods of relatively low monsoonal precipitation. The strongly cemented channel bodies of Unit 2 have been indurated through groundwater and groundwater–pedogenic action in a valley setting. Alpha calcretes predominate in both pedogenic and groundwater carbonate in this part of the Ganga plains.

Wright and Tucker (1991) argued that the preferential development of alpha calcretes in silicate-rich sediments may reflect the "preference of calcites to form bonds with other calcites to displace other grains" (Chadwick and Nettleton, 1990). Alpha fabrics also exhibit evidence of neomorphic spar or microspar, suggesting replacement of finer by coarser crystals (Sehgal and Stoops, 1972; Tandon and Narayan, 1981; Wieder and Yaalon, 1982; Drees and Wilding, 1987). The predominance of alpha fabrics in Kalpi pedogenic calcrete may reflect (a) weak pedogenesis, (b) cohesive bonding of calcite to calcite, and/or (c) replacement and neomorphic aggradation, leading to poor preservation of biological fabrics.

Extensively developed Quaternary calcretes in the semi-arid to arid region of the Thar Desert in northwest India also show predominantly alpha fabrics (Dhir et al., 2004). Taken together with the present study, alpha calcretes appear to predominate in the Quaternary landscapes of northern and western India, where modern rainfall ranges from 200 to 1000 mm/year. Beta fabrics in calcretes formed by soil-forming processes appear to have been weakly developed or poorly preserved, in contrast to studies elsewhere (Nash and McLaren, 2003).

6. Carbon and oxygen isotopic composition of calcrete

Carbon and oxygen isotope data were obtained from carbonates in Units 1, 2, 3 and the lower part of Unit 4 (Table 2). For some rhizoconcretions, nodules, and powdery carbonate, measurements were also made on microdrilled separates of micrite and sparite. Bulk and

Table 2
Stable isotope data for calcretes from Kalpi section

Bulk samples				Microdrilled samples			
Sample no.	Sample description	$\delta^{13}C$ (VPDB)	$\delta^{18}O$ (VPDB)	Sample no.	Sample description	$\delta^{13}C$ (VPDB)	$\delta^{18}O$ (VPDB)
1a: Rhizoconcretions, nodules and carbonate segregations of Unit 1				1c: Micrites corresponding to 1a (microdrills)			
K-IX/1.1	Pedogenic nodule	−3.6	−5.9	K-IX/1.2	Micrite	−5.4	−6.4
K-IX/1.2	Powdery carbonate	−4.1	−6.3	K-IX/1.3	Micrite	−3.5	−6.5
K-IX/1.3	Pedogenic nodule	−4.4	−6.5	K-IX/1.4a	Micrite	−2.6	−6.9
K-IX/1.4a	Rhizoconcretions	−3.3	−6.8	K-IX/1.4b	Micrite	−4.5	−6.4
K-IX/1.4b	Rhizoconcretions	−2.4	−5.4	K-IX/1.5	Micrite	−2.3	−5.7
K-IX/1.5	Reworked Pedogenic nodule	−0.8	−5.4	K-IX/1.6a	Micrite	−2.0	−6.5
K-IX/1.6a	Pedogenic nodule	−2.3	−6.6	Mean		−3.4	−6.4
K-IX/1.6b	Pedogenic nodule	−2.0	−6.0	S.D.		1.4	0.4
K-IX/1.7	Pedogenic nodule	−2.7	−6.5	2b: Micrites corresponding to 2a (microdrills)			
Mean		−2.8	−6.2	K-III/2.1	Micrite	−4.0	−8.4
S.D.		−1.1	−0.5	K-III/2.1b	Micrite	−2.4	−5.5
1b: Groundwater calcretes				K-III/2.1d	Micrite	−4.4	−6.0
K-IX/1.8	Groundwater calcretes	−1.6	−6.5	K-III/2.1d	Micrite with detritus	−3.3	−5.9
K-IX/1.9a	Groundwater calcretes	−3.5	−6.5	Mean		−3.5	−6.5
K-IX/1.9b	Groundwater calcretes	−1.7	−5.7	S.D.		0.9	1.3
Mean		−2.2	−6.3	3b: Micrites corresponding to 3a (microdrills)			
S.D.		1.1	0.5	K-III/3.4a	Micrite	−3.1	−5.9
2a: Rhizocretions, nodules and carbonate segregations (Unit 2)				4b: Micrites of 4a microdrills)			
K-III/2.1	Rhizoconcretions	−3.4	−6.0	K-II/4.5	Micrite	−3.2	−8.1
K-III/2.1a	Rhizoconcretions	−2.9	−5.9	K-II/4.6	Micrite	−2.4	−6.1
K-III/2.1b	Concretion	−3.1	−5.7	K-II/4.8	Micrite	−1.2	−6.6
K-III/2.1d	Rhizoconcretions	−7.3	−6.4	K-II/4.10	Micrite	−2.5	−7.1
K-III/2.2	Powdery carbonate	−5.9	−3.5	K-II/4.13	Micrite	−1.2	−6.0
K-II/2B.1	Pedogenic nodule	−2.7	−5.0	Mean		−2.1	−6.8
K-V/2.1	Rhizoconcretions	−4.40	−5.40	S.D.		−0.8	−0.8
Mean		−4.2	−5.4	6. Micronodule and sparry carbonate			
S.D.		1.7	1.0	K-III/2.1a	Nodule	−4.7	−9.0
3a: Rhizoconcretions, nodules and carbonate segregations (Unit 3)				K-II/4.6	Micritic nodule	−3.3	−6.4
K-II/3.1	Pedogenic nodule	−2.0	−5.3	K-IX/1.4a	Microspar	−3.6	−7.2
K-II/3.2	Pedogenic nodule	−2.5	−7.5	K-III/2.1c	Spar	−2.2	−5.8
K-III/3.1	Pedogenic nodule	−3.0	−5.6	K-III/2.1d	Spar	−5.3	−8.6
K-III/3.4a	Rhizoconcretions	−3.9	−6.7	K-II/4.10	Spar	−2.3	−6.0
K-III/3.4b	Pedogenic nodule	−2.7	−5.1	K-III/2.1a	Crack-filled spar	−2.5	−6.1
Mean		−2.8	−6.0	K-III/3.1	Sparry groundmass	−2.6	−5.5
S.D.		0.7	1.0	K-II/4.4	Sparry groundmass	−1.9	−5.8
4a: Rhizoconcretions, nodules and carbonate segregations (Unit 4)				K-II/4.11	Spar micrite mixed	−1.7	−5.8
K-II/4.1	Pedogenic nodule	−2.0	−5.9	K-IX/1.4a	Veinspar	−2.5	−5.8
K-II/4.2	Pedogenic nodule	−1.5	−5.0	Mean		−3.0	−6.5
K-II/4.3	Pedogenic nodule	−1.9	−6.2	S.D.		1.2	1.2
K-II/4.4	Pedogenic nodule	−1.2	−5.3	5. Veins (bulk samples)			
K-II/4.5	Pedogenic nodule	−1.5	−6.1	K-III/2.1c	Veinfills	−3.10	−5.91
K-II/4.6	Pedogenic nodule	−0.1	−5.5	K-I/2.1	Veinfills	−4.0	−6.2
K-II/4.7	Pedogenic nodule	−0.3	−5.0	K.I/2.2	Veinfills	−5.0	−6.5
K-II/4.8	Pedogenic nodule	−1.3	−6.3	K.I/2.3	Veinfills	−4.7	−6.2
K-II/4.9	Pedogenic nodule	−0.8	−6.1	K.I/2.4	Veinfills	−3.3	−5.5
K-II/4.10	Pedogenic nodule	−1.8	−5.8	K-II/2.1	Veinfills	−3.9	−6.2
K-II/4.11	Pedogenic nodule	−1.7	−6.0	K.II/2.2	Veinfills	−5.6	−6.2
K-II/4.12	Pedogenic nodule	−0.3	−6.1	K-V/2.2	Veinfills	−1.5	−5.7
K-II/4.13	Pedogenic nodule	−1.0	−6.0	K-V/2.3	Veinfills	−4.5	−6.5
K-II/4.14	Pedogenic nodule	−0.8	−5.9	K-V/2.4	Veinfills	−4.5	−5.9
Mean		−1.2	−5.8	Mean		−4.1	−6.1
S.D.		0.6	0.4	S.D.		1.2	0.3

microdrilled samples show a reasonable correspondence (Fig. 7), although there is a considerable average difference in $\delta^{13}C$ values between bulk and microdrilled analyses from the same samples.

For $\delta^{18}O$ values, individual bulk and microdrilled samples range from −9.0‰ to −3.5‰. Mean values for the units show a relatively narrow range, from −5.4‰ to −6.3‰ for bulk samples, and from −6.4‰ to −7.0‰ for microdrilled samples (Table 3). Mean values for the microdrilled carbonates are slightly more negative on average than for the bulk samples. For 17 micritic samples from calcretes, the average difference between $\delta^{18}O$ values for bulk and microdrilled samples is 0.9‰, the microdrilled samples showing more negative values than the bulk samples. The four units have similar isotopic compositions (Fig. 8a, b), and means plus or minus one standard deviations overlap for all four units based on both bulk and microdrilled suites.

For $\delta^{13}C$ values, individual bulk and microdrilled samples range from −7.3‰ to −0.1‰. Mean values for the units show a relatively narrow range, from −1.1‰ to −4.2‰ for bulk samples and from −2.3‰ to −3.8‰ for microdrilled samples (Table 3). For two out of three units, mean values for the microdrilled samples are slightly lower on average than for the bulk samples. For 17 micritic samples from calcretes, the average difference between $\delta^{13}C$ values for bulk and microdrilled samples is 1.6‰. There is a general upward trend towards lower values, with a prominent shift between Units 1 to 3 and Unit 4 (Fig. 8a, c). For the bulk samples, Units 3 and 4 suites do not overlap at one standard deviation.

Cross-plots of $\delta^{13}C$ and $\delta^{18}O$ values (Fig. 9) show a relatively tight cluster, with no apparent stratigraphic trend for $\delta^{18}O$ values through the four units but a clear 2‰ shift in $\delta^{13}C$ values of bulk samples (Fig. 9a) particularly for the pedogenic nodules. There is also some isotopic discrimination between the values for rhizoconcretions, nodules, and veinfills from the same unit (Unit 2) in terms of $\delta^{13}C$ values. There is little apparent isotopic difference between pedogenic and groundwater calcretes. For bulk samples, Unit 2 has the highest spread of data (standard deviation) for both $\delta^{13}C$ and $\delta^{18}O$ values (Table 3).

For organic matter extracted from pedogenic carbonates (Table 4), the $\delta^{13}C$ value in Unit 1 is −21.4‰ ($n=1$), in Unit 2 is −21.5±1‰ ($n=8$), and in Unit 3 is −21.7±1.1‰ ($n=2$).

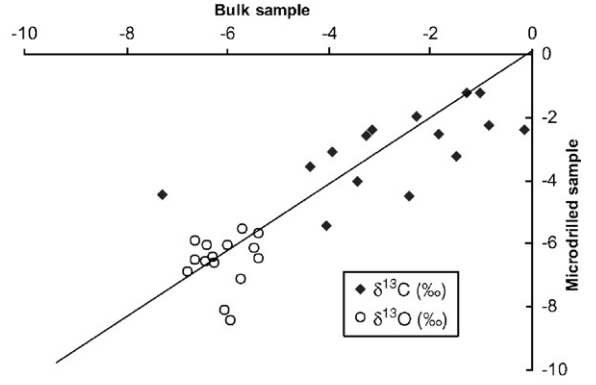

Fig. 7. Comparison of isotopic data from bulk and microdrilled carbonate samples. A good correlation between the two suggests that multiple pedogenic overprinting has not influenced the isotopic values of the carbonates.

7. Paleoprecipitation estimates based on oxygen isotopes

7.1. Reliability of estimates

The $\delta^{18}O$ value of pedogenic carbonate depends on the $\delta^{18}O$ value of soil water and the temperature of carbonate precipitation. Local rainfall infiltrates into the soil to become soil water, and the $\delta^{18}O$ value of soil water should closely reflect the $\delta^{18}O$ value of local rainfall. Because pedogenic carbonate typically precipitates under near-surface conditions, the temperature under which the carbonate precipitated should correspond broadly with the mean annual temperature of the area.

The $\delta^{18}O$ values of Quaternary soil carbonates generally provide a good proxy for soil water chemistry (Cerling, 1984, 1991). However, a caution must be exercised due to the possibilities of overprinting due to multiple phases of pedogenesis (Amundson et al., 1994; Deutz et al., 2001). Our data from the Kalpi section

Table 3
Carbon isotope data for organic matter in calcretes from the Kalpi section

Unit	Sample no.	$\delta^{13}C$ organic
4	KPY-II/4.5	−22.4
	KPY-II/4.5	−20.9
	RZC-1	−21.4
2	KPY-IX-2.1d	−22.0
	KPY-2–1	−21.4
	KPY-2–2	−22.2
	KPY-2–3	−20.8
	KPY-2–4	−23.0
	KPY-2–5	−22.0
	KPY-2–6	−21.7
	KPY-2–7	−21.3
	KPY-2–8	−19.6
1	K-IX/1.4a	−21.4

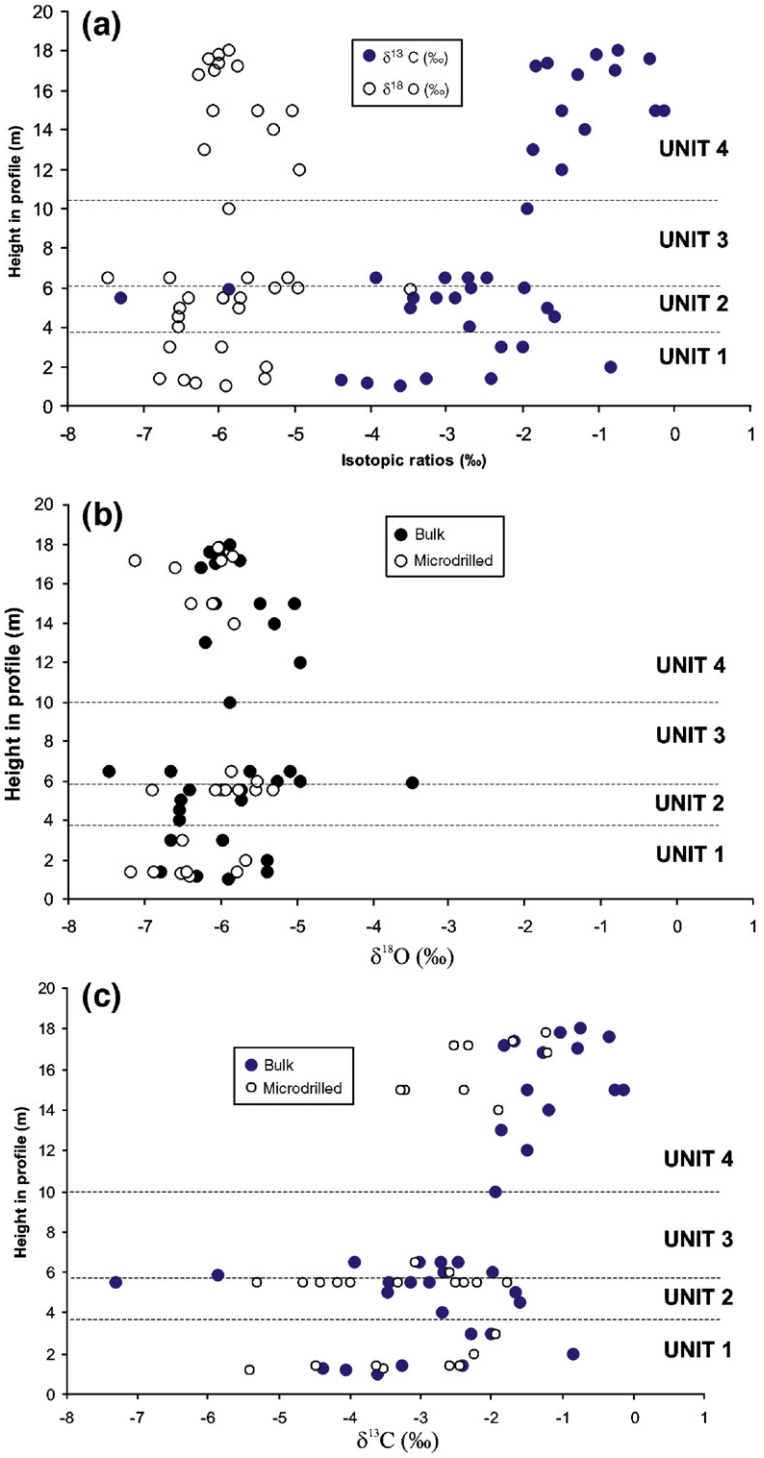

Fig. 8. Stable isotope data for bulk samples showing stratigraphic distribution within Units 1–4 of the Kalpi section. Vein samples are excluded. (a) $\delta^{18}O$ and $\delta^{13}C$ values for all bulk samples. (b) $\delta^{18}O$ values for bulk and microdrilled samples. (c) $\delta^{13}C$ values for bulk and microdrilled samples. The data plotted represents only a part of the section; upper 13 m are not represented; the thickness of Unit 2 is variable and can be up to 4 m.

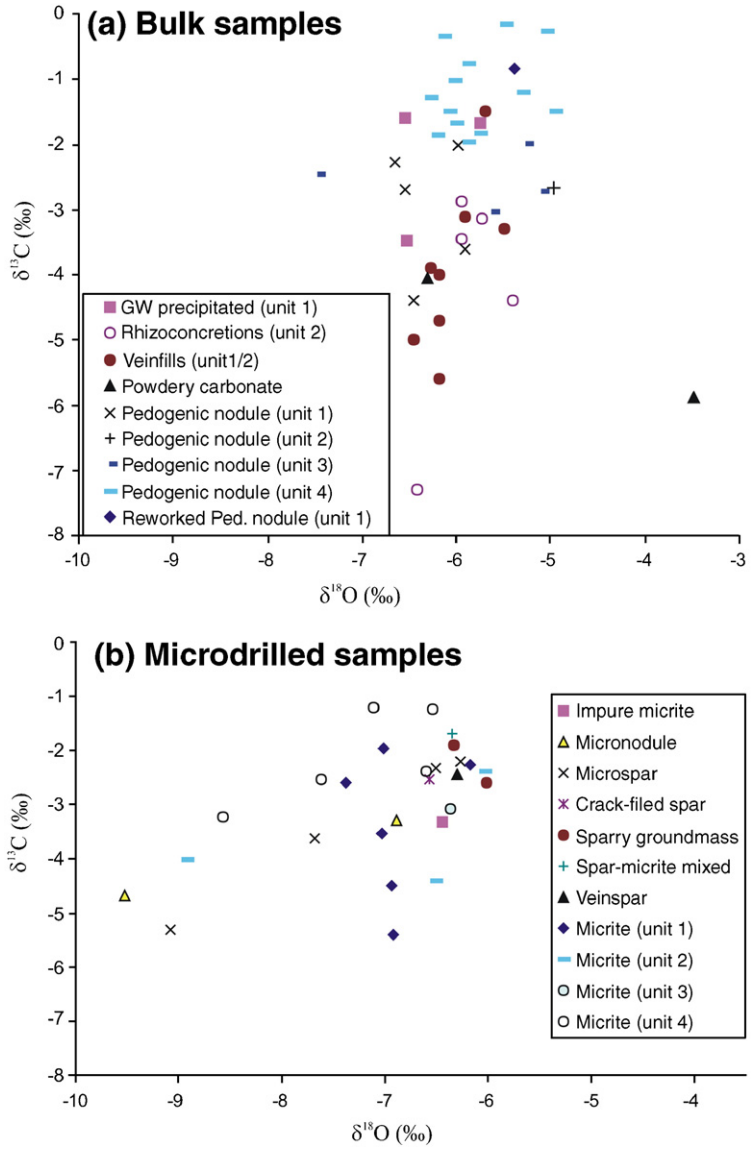

Fig. 9. Stable isotope data. (a) $\delta^{18}O$ vs. $\delta^{13}C$ plot for bulk calcrete samples classified into genetic types. (b) $\delta^{18}O$ vs. $\delta^{13}C$ plot for microdrilled samples from thick sections, classified into genetic types.

clearly demonstrate a very good correspondence between the microdrilled samples and their respective pedogenic feature (Fig. 7), and hence suggests that overprinting is not a major issue here.

Further, in order to use the $\delta^{18}O$ values of Ganga carbonates as a proxy for soil water chemistry, it must be established that the pedogenic carbonate precipitated in isotopic equilibrium with soil water. This can be tested using $\delta^{18}O$ values of young pedogenic carbonate, assuming that the mean annual temperature of the area and the $\delta^{18}O$ value of local rainfall have not changed markedly since their formation. Using the $\delta^{18}O$ value of rainfall near Kanpur as −5.4‰ (based on Krishnamurthy and Bhattacharya, 1991) and mean annual temperature at Kanpur as 25 °C (Singh, 1994), the expected $\delta^{18}O$ value of carbonate precipitating under these conditions can be calculated using the equation:

$$1000\ln\alpha_{\text{water}}^{\text{calcite}} = 2.78 \times 10^6/T^2 - 2.89$$

where $\alpha_{\text{water}}^{\text{calcite}} = (1000+\delta^{18}O_{\text{calcite}})/(1000+\delta^{18}O_{\text{water}})$ (Friedman and O'Neil, 1997).

Table 4
Oxygen and carbon isotopic values in carbonate and organic matter for stratigraphic units of the Kalpi section, expressed as mean±S.D.

Unit	Carbonate type	Facies type	$\delta^{13}C$ in organic matter in nodules	$\delta^{18}O$ in carbonate		$\delta^{13}C$ in carbonate		No. (B/M)
				Bulk	Microdrilled	Bulk	Microdrilled	
4	Rhizoconcretions, nodules+powdery	Floodplain (sand+mud)	n.d.	−5.8±0.4	−6.7±0.77	−1.2±0.6	−2.3±0.9	14/6
3	Rhizoconcretions, nodules+powdery	Floodplain (mud dominated)	−21.7±1.1 (n=2)	−5.8±0.8	n.d.	−3.3±0.6	n.d.	5
2/3	Veins	Tectonic event after deposition of Unit 2	n.d.	−6.1±0.3	n.d.	−4.1±1.2	n.d.	9
2	Rhizoconcretions, nodules+powdery	Plains-fed Channels, with discontinuity above	−21.5±1.0 (n=8)	−5.4±1.1	−7.0±1.6	−4.2±1.9	−3.8±0.9	6/5
1	Rhizoconcretions, nodules+powdery	Floodplain (sand+mud)	−21.4 (n=1)	−6.2±0.5	−6.4±0.4	−2.8±1.1	−3.4±1.4	8/6
1	Groundwater calcrete	Discontinuity at top of Unit 1	n.d.	−6.3±0.5	n.d.	−2.2±1.1	n.d.	3

n.d.=not determined.

The calculated value is −7.3‰. This is very close to the average $\delta^{18}O$ value (−7‰) obtained from carbonate samples from the topmost part of cores from the Ganga Valley at Jagdishpur and Firozpur, close to Kanpur (P. Sanyal, unpublished results). The close agreement between observed and expected $\delta^{18}O$ values strongly suggests that soil carbonate has precipitated in equilibrium with soil water, and that $\delta^{18}O$ values of soil carbonate can be used to estimate paleoprecipitation reliably.

7.2. Paleoprecipitation for the Kalpi area

The mean $\delta^{18}O$ value is −5.8‰ for bulk samples and −6.7‰ for microdrilled samples (pedogenic types, excluding groundwater calcretes and fracture fills) – on average slightly higher than the calculated value for present rainfall in the Kanpur area.

Table 5 lists the average $\delta^{18}O$ values of the pedogenic carbonates for each stratigraphic unit at Kalpi and the computed $\delta^{18}O$ values for soil water for the corresponding units. The computed soil water $\delta^{18}O$ values range from −3.0‰ to −4.3‰ with an average of −3.7‰. Given the fact that for each of the Kalpi stratigraphic units, $\delta^{18}O$ value shows a range of ~2‰ (Fig. 8a, b), these variations are negligible. In low-latitude areas, a 100 mm increase in rainfall causes a decrease in $\delta^{18}O$ of rainwater by 1.5‰ (Yurtsever and Gat, 1981). Given the current average rainfall of 800–1000 mm in the region, the range of variation in $\delta^{18}O$ value documented for each unit may reasonably be inferred to reflect just subtle variations in the amount of monsoonal rainfall over periods of a marine isotope stage or less.

The similarity of values for the four stratigraphic units at Kalpi therefore implies that no large shifts in the amount of precipitation took place in this part of the

Table 5
Computation of paleoprecipitation (soil water) and relative abundance of plant groups

Units	Paleoprecipitation		Plant groups			
	Ave. $\delta^{18}O$ (VPDB) (pedogenic carbonates)	Soil water $\delta^{18}O$ (VSMOW)	Ave. $\delta^{13}C$ (VPDB) (micrites)	% C_4 plants	Ave. $\delta^{13}C$ (VPDB) (organic matter)	% C_4 plants
	Mean annual temperature=25 °C α (water−carbonate)=1.028822		$\delta^{13}C$ value of C_4 plants=−12.5‰ $\delta^{13}C$ value of C_3 plants=−26.5‰ Δ (Carbonate−Soil respired CO_2)=14.4‰			
Unit 4	−5.8±0.4	−3.8	−2.1±0.9	71	−21.6±0.8	35
Unit 3	−5.6±1.1	−3.6	−3.1[a]	64	n.d.	n.d.
Unit 2	−5.0[a]	−3.0	−3.6±1.1	60	−21.6±0.9	35
Unit 1	−6.3±0.3	−4.3	−3.4±1.4	62	−21.4[a]	36
Average	−5.6	−3.7	−3.04	64	−21.5	35

[a] Based on one sample only.

Ganga plains during the period represented by the sample suite – MIS 5 for Units 1 and 2 to MIS 3 for Unit 4. Model calculations for monsoonal precipitation in southern Asia suggest that rainfall was about 35% greater or less than present values at times during MIS 5, and about 15% less than at present during MIS 3 (Prell and Kutzbach, 1987). Thus, there is an apparent discrepancy between the model results and the lack of variation observed in the study area.

8. Vegetation analysis based on carbon isotopes from carbonates

Cerling (1984, 1991) showed that the $\delta^{13}C$ value of soil carbonate can be used to calculate the relative proportion of C_3 and C_4 plants at the time of soil carbonate formation. The computations proposed by Cerling account for depth of nodule formation, atmospheric pCO_2, and isotopic fractionation between soil CO_2 and plant respired CO_2. The net outcome of Cerling's model is that pedogenic carbonate formed at least 25 cm below the land surface should be 14‰ to 17‰ higher than the coeval soil organic matter. Using an average difference of 14.4‰ between the two, one thus derives the $\delta^{13}C$ of the soil carbon from measured $\delta^{13}C$ of soil carbonate. The estimated $\delta^{13}C$ of the soil organic matter, in turn reflects the mixture of C_3 plants (−20‰ to −35‰, average of −26.5‰) and C_4 plants (−10‰ to −16‰, average of −12.5‰), and the relative proportions of the two can be estimated from a simple mass balance calculation (Cerling, 1984). The appearance and expansion of C_4 plants took place ~7 Ma ago based on data from the Siwalik Group of Pakistan and vegetational reconstruction from Siwalik strata (up to about 1 Ma) suggests that lowland vegetation was dominated by C_4 plants (Quade et al., 1989). CAM includes all desert plants, and they have $\delta^{13}C$ values between those of C_3 and C_4 plants.

For the floodplain deposits of Kalpi Units 1, 3 and 4, the $\delta^{13}C$ values for bulk carbonate samples are shown in Table 3. Mean unit values are more negative for Unit 2 than for other units (−4.22‰ for bulk samples, and −3.76‰ for microdrilled samples). Based on micritic samples from Units 1, 2 and 4, the proportion of C_4 plants is estimated at 62%, 60% and 71%, respectively (Table 5). One sample from Unit 3 yielded an estimate of 64%. These estimates suggest that C_4-dominated systems were favored during accumulation of most of the Kalpi strata. The upward trend of higher values within Unit 1 (Fig. 8c) suggests an increased C_4 contribution from the lower floodplain deposits towards the discontinuity at the unit top.

The C_4 plant contribution can also be estimated from the $\delta^{13}C$ value of organic matter in the nodules. For Units 1, 2 and 3, for which data are available (Table 4), there is no real difference in $\delta^{13}C$ values among the different stratigraphic units, and the average value is −21.5‰. The proportion of C_4 plants is therefore estimated at ~35% – a much lower proportion than for carbonate-based estimates. This apparent discrepancy may perhaps be explained by considering the timing of carbon fixation in the system. Organic matter reflects the annual average biomass in the soil – with an especially high contribution probable during the wetter, growing season – whereas carbonate formation may take place during a certain part of year, probably the drier season. The higher proportion of C_4 plants estimated from carbonate isotopes suggests that C_4 plant respiration predominated during carbonate formation, whereas the lower proportion based on organic matter suggests that C_3 plants predominated in the ecosystem during the wetter season and, on average, throughout the year. In a recent work, Stevenson et al. (2005) has shown that $\delta^{13}C$ values in soil organic matter are affected by drought stress (seasonality), apart from the primary factors of depositional processes and turnover rate of carbon. On the other hand, the primary determinants of the $\delta^{13}C$ values of pedogenic carbonates are the soil CO_2 isotopic composition, the amount and isotopic signature of diffused atmospheric CO_2 and temperature (Cerling, 1984). We therefore infer that seasonality exerted a noticeable influence on the C_3–C_4 system of the Kalpi section in the Ganga plains.

Alternate explanations for the discrepancy of C_4 plant estimates from the pedogenic carbonates and organic matter include (a) subsequent diagenesis of pedogenic nodules, (b) selective preservation of ligins (generally being 1–3‰ more negative than bulk organic matter) and (c) The assumption of 14–17‰ difference between soil carbonate and soil organic matter is not valid. The explanation (a) is ruled out mainly due to close correspondence between bulk and microdrilled samples. The explanations (b) and (c) need to be tested using data from other sections in the region should further resolve this issue.

9. Reconciling climate model predictions with Kalpi isotopic data

Units 1 to 4 at Kalpi span an age range from about 119±12 ka to 47.1±3.4 ka. As noted above, the sampled interval probably represents a period of 60,000 to 90,000 years during Marine Isotope Stages 3 to 5. Major changes in monsoonal precipitation were

inferred from climate modeling for this period (Fig. 2; Prell and Kutzbach, 1987; Overpeck et al., 1996), and are supported by a variety of field-based evidence in southern Asia.

The present analysis was designed to test for shifts in paleoprecipitation and vegetation type at Kalpi, where the stratal record spans periods of known strong precipitation variation. Surprisingly, however, such shifts are not apparent from our data. The oxygen isotope record suggests that the area did not experience major changes in precipitation during this period. In a given monsoonal state, there is some variability (~10%) around the mean precipitation value, and our Kalpi data seems to have identified only this level of variability. The carbon isotope record also shows little systematic change, with the inference of mixed (C_3–C_4 type) vegetation and a predominance of C_4 plants. The record does, however, suggest a modest increase in the proportion of C_4 plants in the upper part of Unit 1 and in Unit 4, and a higher C_3 (riparian?) plant contribution in the channel deposits of Unit 2.

Some possible explanations may be offered for this apparent discrepancy between model and isotopic results:

(a) The climate modeling is based on regional (global) considerations, and may be inaccurate for this local area. Field data in Rajasthan suggest that precipitation was double of the present values about 10 ka ago, but model data suggest only about 30% change (Swain et al., 1983 compared with Prell and Kutzbach, 1987). Given such a divergence between regional models and local field-based estimates, it is possible that the variation in precipitation for the southern Ganga plains was considerably different (in this case less pronounced) than the models would suggest. Possible contributing factors might include the migration of the Inter-Tropical Convergence Zone, which could have exerted an important local effect on precipitation patterns (Goodbred, 2003), and the influence of the Northeast Monsoon (Enzel et al., 1999).

(b) The Ganga plains near Kalpi may not have been close to a threshold for change in vegetation type, even if precipitation showed considerable variation. Alternatively, vegetation change, being of low intensity and subject to considerable local variation, may not reflect adequately major changes in precipitation. These suggestions are difficult to test in view of the lack of $\delta^{18}O$ value evidence for precipitation fluctuations.

(c) The sampled strata represent periods of floodplain aggradation. Few samples – principally from groundwater-cemented discontinuity surfaces – represent degradational episodes. Thus, the section may have selectively preserved the periods during which precipitation and river discharge were relatively high, and floodplain accumulation was enhanced, leading to the recording of a restricted precipitation range. Additionally, if aggradation was rapid, thick stratal intervals may represent relatively short periods, and much of the time represented by the overall section may be missing from the sample suite. The upward change in $\delta^{13}C$ value in Unit 1 suggests that plant type changed as the floodplain ceased to aggrade, leading to carbonate cementation of degradational surfaces.

(d) The strata include channel deposits (Unit 2). Unit 2 yields a relatively high proportion of C_3 vegetation and an unusually great variability in isotopic composition. The availability of water may have promoted the growth of C_3 (riparian) vegetation in addition to C_4 vegetation, resulting in a varied, mixed isotopic sample suite. Both pedogenic and groundwater carbonates are present in the unit, perhaps resulting in a varied isotopic system. In addition to the ambient rainwater, the channels may have provided water with a more varied composition, for example from local groundwater systems.

(e) The isotopic values may reflect in part the timing of fixation of carbon and oxygen in the monsoonal, strongly seasonal setting of the Ganga plains. This is demonstrated by the contrast between vegetation types inferred from analysis of carbonate and organic matter from the same nodules. Seasonal effects may have contributed to some variability in the data set.

(f) Diagenetic overprinting of the original carbonate may have blurred the results. Although this cannot be entirely ruled out, the pedogenic samples were composed predominantly of micrite (rather than microspar or coarser sparite which might indicate some recrystallization). Where possible, comparisons were made between micrite-rich components. Also, the broad similarity between bulk and microdrilled samples suggests that later diagenetic effects were modest.

(g) The age model for the strata may be inaccurate. However, where they could be compared, our OSL and TL dates showed a close correspondence, and our ages are broadly comparable with

those of Srivastava et al. (2003). For other sections in the Ganga plains, good correspondence was obtained between OSL and radiocarbon dates (Gibling et al., 2005).

Although none of the above explanations can be entirely confirmed or ruled out, we tentatively suggest that the lack of evidence for climatic and vegetation change reflects three principal factors: preferential preservation of aggradational periods; the local predominance of riparian vegetation which would yield a record of mixed plant groups; and seasonal effects (explanations c, d, and e). These factors are related to the local floodplain setting or to local climatic seasonality. Departure of local precipitation fluctuations from the climatic model (much lower than predicted) needs further testing because strong isotopic excursions have been documented in other parts of the Himalayan Foreland Basin (see Section 10).

An additional factor is the CO_2 concentration in the atmosphere. The physiology of C_4 plants suggests that they are favored under conditions of low CO_2 concentration (Cerling et al., 1997). Estimation of atmospheric CO_2 concentration from the Vostok ice core for the last 100 ka shows a decrease from 290 ppmV to 180 ppmV up to LGM time (Barnola et al., 1991), and atmospheric levels should have been decreasing through the studied interval. Modern C_4 plants are favoured by aridity and a high degree of seasonality. Thus, a combination of increase in aridity and lowering of CO_2 from Units 1 and 2 to Unit 4 may explain in part the increase in abundance of C_4 plants through the period of MIS 5 to MIS 3. Monsoon variation along with lowering of atmospheric CO_2 concentration was cited as the cause for the appearance and expansion of C_4 plants documented in the Siwalik Group (Sanyal et al., 2004). However, the appearance of abundant C_4 plants in the Siwalik Group varied by up to 2 Myr locally (Quade et al., 1989; Sanyal et al., 2004, 2005), suggesting that local controlling factors (in addition to global CO_2 concentration) were of considerable importance.

10. Spatial variation in climatic parameters in the Himalayan Foreland Basin

Data on the stable isotope composition of continental carbonates and shells from the Ganga plains is meager (Pendall and Amundson, 1990; Alam et al., 1997; Srivastava, 2001; Sharma et al., 2004). Considering the wide variations in temperature and precipitation patterns that exist over this vast area (~1 million km^2), it is important to understand whether the stable isotope composition of the continental carbonates is a useful proxy for climate and vegetation type. Such an assessment is needed both for the modern context and for the Holocene and late Pleistocene context. Alam et al. (1997) and Srivastava (2001) concluded that the isotope composition of Pleistocene and Holocene pedogenic carbonates is a useful paleoclimate indicator for the Ganga plains. In a recent comprehensive study of stable isotopes of shells and organic matter (coupled with elemental geochemistry and pollen analysis) of a sediment profile from Sanai Tal (lake) on the central Ganga plain, Sharma et al. (2004) inferred that 'millennium-scale climate oscillations …correlate well with records from other parts of the Indian subcontinent indicating that the recorded changes are an expression of broad scale, probably global and climatic change'. This latter study spans the last 15 ka.

In Fig. 10, we plot our data together with pedogenic carbonate data from Middle–Upper Pleistocene strata of northwestern Bangladesh (Alam et al., 1997) and data from Holocene strata between the Ramganga and Rapti rivers of the eastern Ganga plains (Srivastava, 2001). Our data are more tightly clustered than those of the other two data sets. Both show subsets with significant separation or only narrow overlap, with sharp changes in the isotopic composition. They appear to represent a wide range of monsoonal conditions, although the lack of age data restricts a fuller analysis. Alam et al. (1997) estimated shifts in C_4 percentage from 1–12% to 92–97% and from 8–28% to 94–99% for sample groups. The data of Srivastava (2001) for Type 1 calcretes associated with old soils (estimated at 6500–13,500 years BP) show large variations in $\delta^{13}C$ value from +1.6‰ to −6.9‰. The youngest Type 3 calcrete $\delta^{13}C$ values, however, cluster in a narrow range between +0.3‰ and +1.8‰. The $\delta^{18}O$ values for these two groups of calcrete vary from −6.1‰ to −10.5‰ (Srivastava, 2001).

The available data suggest that strong monsoon-induced vegetational shifts from C_3-dominated to C_4-dominated are apparent for the Ganga–Brahmaputra delta and eastern Ganga plains during the Pleistocene and Holocene, respectively. Variation in the oxygen isotopic compositions of pedogenic carbonates for these data subsets is typically ~2‰, except for the Type 2 calcrete of the Ramganga–Rapti area. Similar shifts have yet to be demonstrated for interfluve palaeosol carbonates in the southern Ganga plains

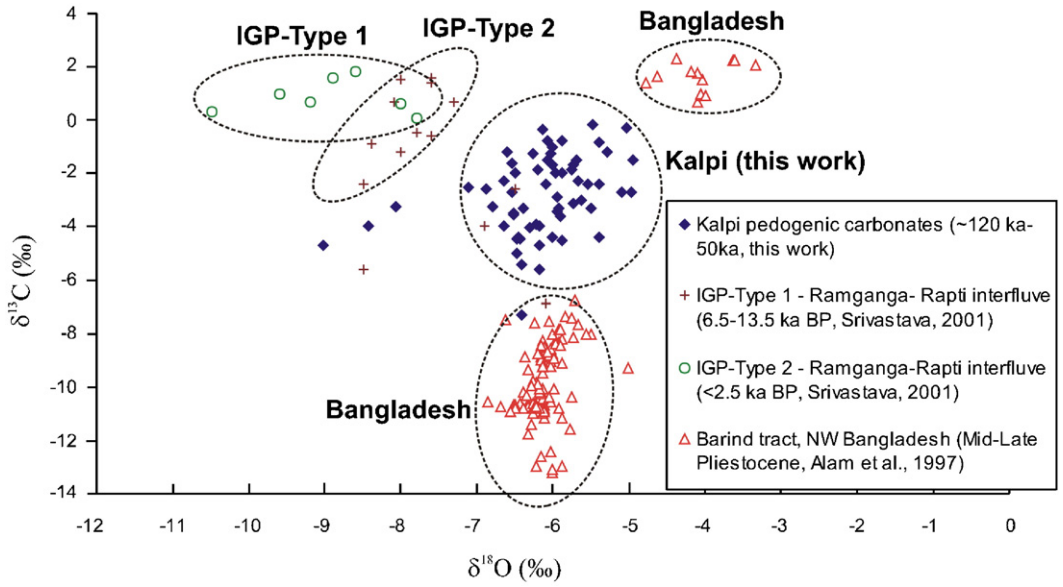

Fig. 10. Comparison of carbon and oxygen isotope data for Kalpi carbonates with those from other parts of the Ganga plains (Srivastava, 2001) and Bangladesh (Alam et al., 1997).

(Kalpi section) through the MIS 3 to MIS 5 interval. Further tests are needed to determine whether the apparent lack of isotope excursions in the southern plains reflects local and seasonal factors or whether it forms part of a systematic pattern of monsoon intensity through space and time in southern Asia.

11. Conclusions

1. Pedogenic, groundwater, and mixed pedogenic–groundwater calcretes are common within Late Quaternary discontinuity-bounded alluvial sequences of the southern Ganga plains, India. Calcrete nodules and rhizoconcretions are present within floodplain aggradation deposits, which correspond to periods of relatively high monsoonal precipitation and river discharge. The deposits are truncated by degradational surfaces (discontinuities) that have several meters of relief. These irregular surfaces are cemented with carbonate, with caps of reworked nodules, and correspond with periods of relatively low precipitation. Mixed groundwater and pedogenic calcretes are present in the deposits of small interfluve channels. The stratigraphic distribution of carbonate types is linked to the alluvial architecture, formed in response to monsoon-driven rhythms of aggradation and degradation.
2. Calcretes of all types show predominantly alpha fabrics characterized by floating textures, shrinkage crack fills, and grain coatings. Similar fabrics characterise calcretes developed in fluvial and desert landscape across northern India.
3. $\delta^{13}C$ and $\delta^{18}O$ values of 61 calcrete samples show relatively little variation in precipitation and vegetation types through the 18 m sampled interval at Kalpi. Bulk and microdrilled samples show relatively similar isotopic compositions. Floodplain deposits were vegetated with a mixture of C_4 and C_3 plants (predominantly C_4). This apparent lack of variation is surprising because the sampled interval represents at least 60,000 years of Marine Isotope Stages 3–5, during which climate models (Prell and Kutzbach, 1987) suggest that Asia experienced radical fluctuations in monsoon intensity and precipitation. In contrast, strong shifts in isotopic patterns are observed in Holocene deposits of the eastern Ganga plains and in Pleistocene deposits in Bangladesh. Incomplete age and climate information cannot be ruled out for the Kalpi setting. However, the section may have preferentially preserved aggradational strata that represent relatively active monsoonal periods. Additionally, mixing of drier floodplain (C_4) and riparian (C_3) vegetation may explain some of the apparent lack of variation. In support of these inferences, a higher proportion of C_3 plants was associated with channel deposits, as well as with the lower parts of aggradational to degradational rhythms.
4. In comparison to data from carbonates, isotopic analysis of organic matter from floodplain pedogenic

nodules suggests a much greater contribution from C_3 plants. The preserved organic matter may reflect the annual average biomass in the soil and the effects of the wetter growing season, with a higher proportion of C_3 plants, whereas carbonate formation may have taken place mainly during the drier season when respiration of C_4 plants made a more important contribution. In interfluve settings such as Kalpi, seasonality may strongly affect the C_3–C_4 system, with preferential preservation of only part of the biomass, enhancing the apparent uniformity of the system.

5. The Kalpi section contains an unusually wide range of pedogenic and groundwater carbonate, associated with a Late Quaternary floodplain (interfluve) succession. The section constitutes one of the most complete and fully dated exposures in the Ganga plains, and the carbonates can be placed in a reliable stratigraphic context, spanning at least 60,000 years and part or all of three marine isotope stages. Because of this unusually high degree of stratigraphic precision, our analysis was designed to test the effects of major monsoonal variations on an interfluve system. Nevertheless, the isotopic results are difficult to interpret, and the isotopic systems appear to have been subject to local influences, including short-term aggradation, local vegetational biomes, and seasonal effects. Some of these effects may have caused preservational bias. Alternatively, regional climatic models may not adequately represent local climatic patterns. Further tests are needed to determine whether southern Ganga plains successions elsewhere record a more consistent correlation between climatic variation and carbonate systems.

Acknowledgements

The manuscript was conceived while RS and SKT were at the Institute of Mineralogy and Geochemistry at Karlsruhe, Germany supported by Alexander von Humboldt foundation and INSA–DFG, respectively, during the summer of 2002. The stratigraphic work in the region was supported by a grant from Department of Science and Technology, Government of India and from a grant to MRG from the Natural Sciences and Engineering Research Council of Canada. We thank all these institutions and organizations for their support. We sincerely thank Gesine Peruss at IMG, Karlsruhe for her help in generating isotope data, and for geochemical analysis. We are thankful to the Steven G. Driese, David A. Budd and an anonymous reviewer as well as the editor for their very constructive comments. The paper has benefited immensely from these comments.

References

Agarwal, A.K., Rizvi, M.H., Singh, I.B., Kumar, A., Chandra, S., 1992. Carbonate deposits in Ganga Plain. In: Singh, I. (Ed.), Gangetic Plain: Terra Incognita. Geology Department, Lucknow University, pp. 35–43.

Alam, M.S., Keppens, E., Paepe, R., 1997. The use of oxygen and carbon isotope composition of pedogenic carbonates from Pleistocene palaeosols in NW Bangladesh, as palaeoclimatic indicators. Quaternary Science Reviews 16, 161–168.

Amundson, R., Francovizcaino, E., Graham, R.C., DeNiro, M., 1994. The relationship of precipitation seasonality to the flora and stable-isotope chemistry of soils in the Vizcaino Desert, Baja-California, Mexico. Journal of Arid Environments 28 (4), 265–279.

Anderson, D.M., Prell, W.L., 1993. A 300 kyr record of upwelling off Oman during the Late Quaternary. Evidence of the Asian Southwest Monsoon. Paleoceanography 8, 193–208.

Andrews, J.E., Tandon, S.K., Dennis, P.F., 1995. Concentration of carbon dioxide in the Late Cretaceous atmosphere. Journal of the Geological Society (London) 152, 1–3.

Bajpai, V.N., Gokhale, K.V.G.K., 1986. Hydrogeomorphic classification of the Marginal Gangetic Alluvial plain in Uttar Pradesh, India, using satellite imageries. Journal of Geological Society of India 28 (1), 9–20.

Bal, L., 1975. Carbonate in soils: a theoretical consideration on, and proposal for its fabric analysis: I and II. Netherlands Journal of Agricultural Science, 23: 18–35, 163–176.

Barnola, J.M., Pimienta, P., Raynaud, D., Korotkevich, Y.S., 1991. CO_2 climate relationship as deduced from the Vostok ice core: a re-examination based on new measurements and on a re-evaluation of the air dating. Tellus 43B (2), 83–91.

Brewer, R., 1964. Fabric and Mineral Analysis of Soils. John Wiley and Sons, New York.

Budd, D.A., Pack, S.M., Fogel, M.L., 2002. The destruction of paleoclimatic isotopic signals in Pleistocene carbonate soil nodules of western Australia. Palaeogeography, Palaeoclimatology, Palaeoecology 188, 249–273.

Bullock, P., Fedoroff, M., Jongerius, A., Stoops, G., Tursina, T., 1985. Handbook for Soil Thin Section Description.

Cerling, T.E., 1984. The stable isotopic composition of modern soil carbonate and its relationship to climate. Earth and Planetary Science Letters 71, 229–240.

Cerling, T.E., 1991. Carbon dioxide in the atmosphere: evidence from Mesozoic palaeosols. American Journal of Science 291, 377–400.

Cerling, T.E., Quade, J., 1993. Stable carbon and oxygen isotopes in soil carbonates. In: Swartz, P., Lohmann, K., McKenzie, J. (Eds.), Continental Isotopic Indicators of Climate. AGU Monograph.

Cerling, T.E., Quade, J., Wang, Y., Bowman, J.R., 1989. Carbon isotopes in soils and palaeosols as ecology and palaeoecology indicators. Nature 34, 138–139.

Cerling, T.E., Harris, M.J., MacFadden, J.B., Leaky, G.M., Quade, J., Eisenmann, V., Ehleringer, R.J., 1997. Global vegetational change through the Miocene/Pliocene boundary. Nature 389, 153–158.

Chadwick, O., Nettleton, W.D., 1990. Micromorphological evidence of adhesive and cohesive forces in soil cementation. In: Dauglas, L. (Ed.), Soil Micromorphology: A Basic and Applied Science. Elsevier, pp. 207–212.

Clemens, S., Prell, W., Murray, D., Shimmield, G., Weedon, G., 1991. Forcing mechanisms of the Indian Ocean monsoon. Nature 353, 720–725.

Dhir, R.P., Tandon, S.K., Sareen, B.K., Ramesh, R., Rao, T.K.G., Kailath, A.J., Sharma, N., 2004. Calcretes in the Thar Desert:

genesis, chronology and paleoenvironment. Proceedings of the Indian Academy of Sciences. Earth and Planetary Sciences 113 (3), 473–515.

Deutz, P., Montanez, I.P., Monger, H.C., Morrison, J., 2001. Morphology and isotope heterogeneity of Late Quaternary pedogenic carbonates: implications for paleosol carbonates as paleoenvironmental proxies. Palaeogeography, Palaeoclimatology, Palaeoecology 166 (3–4), 293–317.

Drees, L., Wilding, L., 1987. Micromorphologic record and interpretations of carbonate forms in the Rolling Plains of Texas. Geoderma 40, 157–175.

Enzel, Y., Ely, L.L., Mishra, S., Ramesh, R., Amit, R., Lazar, B., Rajaguru, S.N., Baker, V.R., Sandler, A., 1999. High-resolution Holocene environmental changes in the Thar Desert, northwestern India. Science 284, 125–128.

Esteban, M., Klappa, C., 1983. Subaerial exposure environment. Memoir-American Association of Petroleum Geologists 33, 1–54.

Friend, P.F., Moody-Stuart, M., 1972. Sedimentation of the Wood Bay Formation (Devonian) of Spitsbergen: regional analysis of a late orogenic basin. Norsk Polarinstitutt 157, 1–77.

Friedman, I., O'Neil, J., 1997. Compilation of stable isotopic fractionation factors of geochemical interest. In: Fleischer, M. (Ed.), Data of Geochemistry. U.S. Geological Survey. 12 pp.

Ghosh, P., Padia, J.T., Mohindra, R., 2004. Stable isotopic studies of palaeosol sediment from Upper Siwalik of Himachal Himalaya: evidence for high monsoonal intensity during late Miocene? Palaeogeography, Palaeoclimatology, Palaeoecology 206, 103–114.

Gibling, M.R., Tandon, S.K., Sinha, R., Jain, M., 2005. Discontinuity-bounded alluvial sequences of the southern Gangetic plains, India: aggradation and degradation in response to monsoonal strength. Journal of Sedimentary Research 75, 373–389.

Goodbred Jr., S.L., 2003. Response of the Ganges dispersal system to climate change: a source-to-sink view since the last interstade. Sedimentary Geology 162, 83–104.

Goodbred, S.L., Kuehl, S.A., 2000. The significance of large sediment supply, active tectonism, and eustasy on margin sequence development: Late Quaternary stratigraphy and evolution of the Ganges–Brahmaputra delta. Sedimentary Geology 133, 227–248.

Goudie, A.S., 1983. Calcrete. In: Goudie, A.S., Pye, K. (Eds.), Chemical Sediments and Geomorphology, pp. 93–131.

Kale, V.S., 1998. Monsoon floods in India: a hydro-geomorphic perspective. Memoir-Geological Society of India 41, 229–256.

Klappa, C., 1978. Biolithogenesis *Microcodium*: elucidation. Sedimentology 25, 489–522.

Klappa, C., 1979. Calcified filaments in Quaternary calcretes: organo-mineral interactions in the subaerial vadose environment. Journal of Sedimentary Petrology 49, 955–968.

Klappa, C., 1983. A process–response model for the formation of pedogenic calcretes. In: Wilson, R.C.L. (Ed.), Residual Deposits. Spec. Publ.-Geol. Soc. Lond., pp. 211–220.

Krishnamurthy, R.V., Bhattacharya, S.K., 1991. Stable oxygen and hydrogen isotope ratios in shallow ground waters from India and a study of role of evapotranspiration in the Indian Monsoon. In: Taylor Jr., H.P., O'Neil, J., Kaplan, I.R. (Eds.), Stable Isotope Geochemistry: A Tribute to Samuel Epstein. Special Publication-Geochemical Society, vol. 3, pp. 187–193.

Mack, G.H., Cole, D.R., Trevino, L., 2000. The distribution and discrimination of shallow, authigenic carbonate in the Pliocene–Pleistocene Palomas Basin, southern Rio Grande rift. Geological Society of America Bulletin 112 (5), 643–656.

Monger, H.C., Daughtery, L.A., Lindemann, W.C., Liddell, C.M., 1991. Microbial precipitation of pedogenic calcite. Geology 19, 997–1000.

Mora, C.I., Driese, S.G., Colarusso, L.A., 1996. Middle to Late Palaeozoic atmospheric CO_2 levels from soil carbonate and organic matter. Science 271, 1105–1107.

Mount, J., Cohen, A., 1984. Petrology and geochemistry of rhizoliths from Plio-Pleistocene fluvial and marginal lacustrine deposits, East Lake Turkana, Kenya. Journal of Sedimentary Petrology 54, 263–275.

Nagtegaal, P.J.C., 1969. Microtextures in recent and fossil caliches. Leidse Geologische Mededelingen 42, 131–142.

Narula, P.L., Acharyya, S.K., Banerjee, J.e., 2000. Eastern Nepal Himalaya and Indo-Gangetic Plains of Bihar. Seismotectonics Atlas of India and its Environs. Geological Survey of India, pp. 26–27.

Nash, D.J., McLaren, S.J., 2003. Kalahari valley calcretes: their nature, origins and environmental significance. Quaternary International 111, 3–22.

Nash, D.J., Smith, R.F., 2003. Properties and development of channel calcretes in a mountain catchment, Tabernas Basin, southeast Spain. Geomorphology 50, 227–250.

Overpeck, J., Anderson, D., Trumbore, S., Prell, W., 1996. The southwest Indian monsoon over the last 18000 years. Climate Dynamics 12, 213–225.

Pascoe, R.D., 1917. Early history of the Indus–Brahmaputra and Ganges. Quarterly Journal of the Geological Society of London 76, 136.

Pendall, E., Amundson, R., 1990. The stable isotope chemistry of pedogenic carbonate in an alluvial soil from the Punjab. Soil Science 149, 199–211.

Prell, W.L., Kutzbach, J.E., 1987. Monsoon variability over the past 150,000 years. Journal of Geophysical Research 92, 8411–8425.

Prell, W.L., Kutzbach, J.E., 1992. Sensitivity of the Indian monsoon to forcing parameters and implications for its evolution. Nature 360, 647–652.

Quade, J., Roe, L.J., 1999. The stable-isotope composition of early ground-water cements from sandstone in Paleoecological reconstruction. Journal of Sedimentary Research 69 (3), 667–674.

Quade, J., Cerling, T.E., Bowman, J.R., 1989. Development of Asian monsoon revealed by marked ecological shift during the latest Miocene in the Northern Pakistan. Nature 342, 163–166.

Sanyal, P., Bhattacharya, S.K., Kumar, R., Ghosh, S.K., Sangode, S.J., 2004. Mio-Pliocene monsoonal record from Himalayan Foreland Basin (Indian Siwalik) and its relation to vegetational change. Palaeogeography, Palaeoclimatology, Palaeoecology 205, 23–41.

Sanyal, P., Bhattacharya, S.K., Kumar, R., Ghosh, S.K., Sangode, S.J., 2005. Palaeovegetational reconstruction in late Miocene: a case study based on early diagenetic carbonate cement from the Indian Siwalik. Palaeogeography, Palaeoclimatology, Palaeoecology 228 (3–4), 245–259.

Sehgal, J.L., Stoops, G., 1972. Pedogenic calcite accumulations in arid and semi-arid regions of the Indo-Gangetic alluvial plain of Erstwhile Punjab (Punjab). Geoderma 8, 59–72.

Sharma, S., Joachimski, M., Sharma, M., Tobschall, H.J., Singh, I.B., Sharma, C., Chauhan, M.S., Morgenroth, G., 2004. Late glacial and Holocene environmental changes in Ganga plain, Northern India. Quaternary Science Reviews 23, 145–159.

Singh, R.L., 1994. India: A Regional Geography. National Geographical Society of India, Varanasi.

Singh, I.B., Sharma, S., Sharma, M., Srivastava, P., Rajagopalan, G., 1999. Evidence of human occupation and humid climate of 30 ka in the alluvium of southern Ganga plain. Current Science 76 (7), 1022–1026.

Sinha, R., Khanna, M., Jain, V., Tandon, S.K., 2002. Mega-geomorphology and sedimentation history of parts of the Ganga–Yamuna plains. Current Science 82 (5), 562–566.

Sinha, R., Tandon, S.K., Gibling, M.R., Bhattacharjee, P.S., Dasgupta, A.S., 2005a. Late Quaternary geology and alluvial stratigraphy of the Ganga basin. Himalayan Geology 26 (1), 223–240.

Sinha, R., Gibling, M.R., Tandon, S.K., Jain, V., Dasgupta, A.S., 2005b. Quaternary stratigraphy and sedimentology of the Kotra section on the Betwa river, Southern Gangetic plains, Uttar Pradesh. Journal of the Geological Society of India 65, 441–450.

Srivastava, P., 2001. Paleoclimatic implications of pedogenic carbonates in Holocene soils of the Gangetic plains, India. Palaeogeography, Palaeoclimatology, Palaeoecology 172, 207–222.

Srivastava, P., Parkash, B., Sehgal, J.L., Kumar, S., 1994. Role of neotectonics and climate in development of the Holocene geomorphology and soils of the Gangetic Plains between the Ramganga and Rapti rivers. Sedimentary Geology 94, 129–151.

Srivastava, P., Singh, I.B., Sharma, M., Singhvi, A.K., 2003. Luminescence chronometry and Late Quaternary geomorphic history of the Ganga Plain, India. Palaeogeography, Palaeoclimatology, Palaeoecology 197, 15–41.

Stevenson, B.A., Kelly, E.F., McDonald, E.V., Busacca, A.J., 2005. The stable carbon isotope composition of soil organic carbon and pedogenic carbonates along a bioclimatic gradient in the Palouse region, Washington State, USA. Geoderma 124 (1–2), 37–47.

Swain, A.M., Kutzbach, J.E., Hastenrath, S., 1983. Estimates of Holocene precipitation for Rajasthan, India, based on pollen and lake-level data. Quaternary Research 19, 1–17.

Tandon, S.K., Friend, P., 1989. Near surface shrinkage and carbonate replacement processes, Arran Cornstone Formation, Scotland. Sedimentology 36, 1113–1126.

Tandon, S.K., Kumar, S., 1999. Semi-arid/arid zone calcretes: a review. In: Singhvi, A.K., Derbyshire, E. (Eds.), Paleoenvironmental Reconstruction in Arid Lands. Oxford-IBH, New Delhi, pp. 109–152.

Tandon, S.K., Narayan, D., 1981. Calcrete conglomerate, a case-hardened conglomerate and cornstone – a comparative account of pedogenic and non-pedogenic carbonates from the continental Siwalik Group, Punjab, India. Sedimentology 28, 353–367.

Tandon, Varshney, 1991. S.K. Tandon and S.K. Varshney, Origin of selective carbonate cemented (concretionary) layers within multi-storied sandstone bodies of the Neogene Middle Siwalik Subgroup, NW Himalaya, India, Abstract, Birbal Sahni Birth Centenary Symposium on the Siwalik Basin, WIHG, Dehra Dun, India: 45.

Tandon, S.K., Andrews, J.E., Sood, A., Mittal, S., 1998. Shrinkage and sediment supply control on multiple calcrete profile development: a case study from the Maastrichtian of central India. Sedimentary Geology 119, 25–45.

Verrecchia, E., Verrecchia, K., 1994. Needle fiber calcite: a critical review and a proposed classification. Journal of Sedimentary Research, A 64, 650–664.

Waelbroeck, C., Labeyrie, L., Michel, E., Duplessy, J.C., Mcmanus, J.F., Lambeck, K., Balbon, E., Labracherie, M., 2002. Sea-level and deep water temperature changes derived from benthic foraminifera isotopic records. Quaternary Science Reviews 21, 295–305.

Watts, N.L., 1978. Displacive calcite: evidence from recent and ancient calcretes. Geology 6, 699–703.

Wieder, M., Yaalon, D., 1982. Micromorphological fabrics and development stages of carbonate nodular forms related to soil characteristics. Geoderma 28, 203–220.

Williams, M.A.J., Clarke, M.F., 1995. Quaternary geology and prehistoric environments ion the Son and Belan Valleys, North Central India. Memoir-Geological Society of India 32, 282–308.

Wright, V.P., Tucker, M.E., 1991. Calcretes, reprint series. International Association of Sedimentologists 1–22.

Yurtsever, Y., Gat, J., 1981. Atmospheric waters. In: Gat, J.R., Gonfiantini, R. (Eds.), Stable Isotope Hydrology: Deuterium and Oxygen-18 in the Water Cycle. Technical Report Series, vol. 210. IAEA, pp. 103–142.